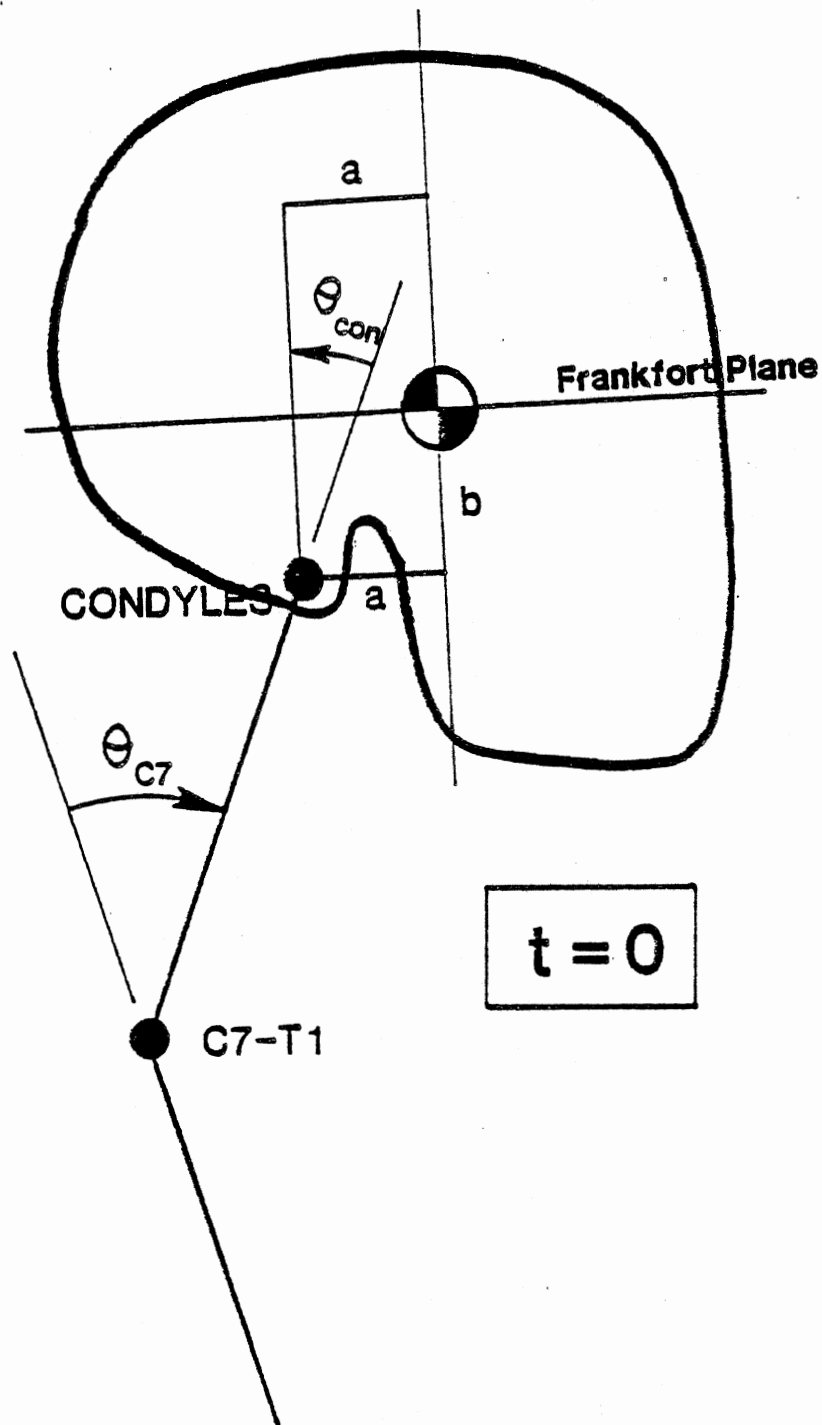


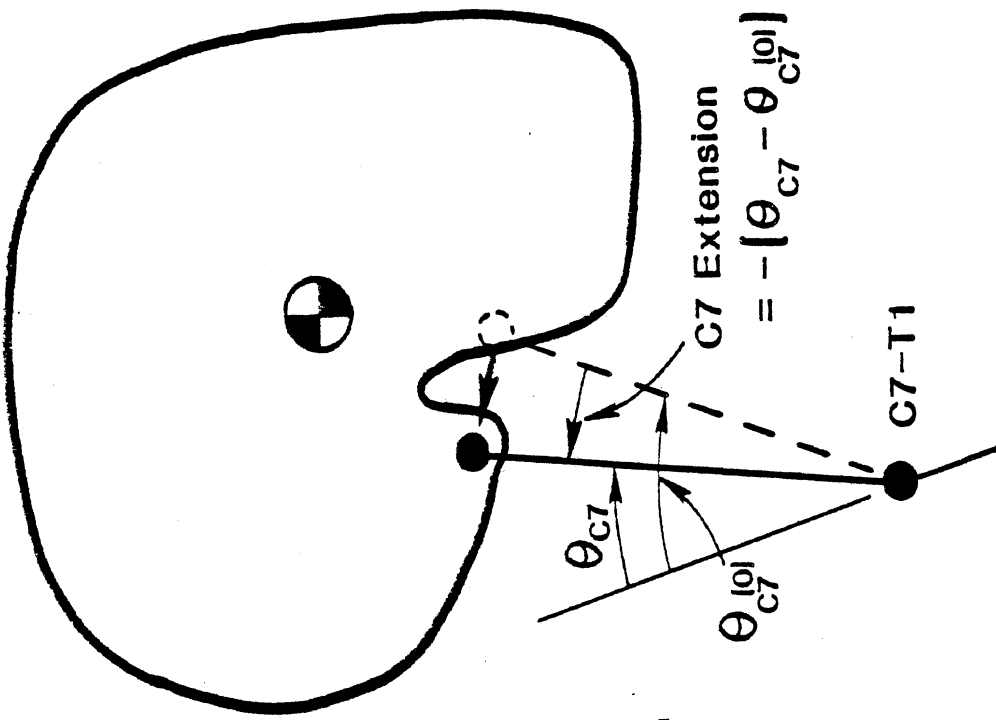
Figure 1. The Two-Joint Neck in the MVMA 2-D CVS Model



Angular deflection at each joint = 0

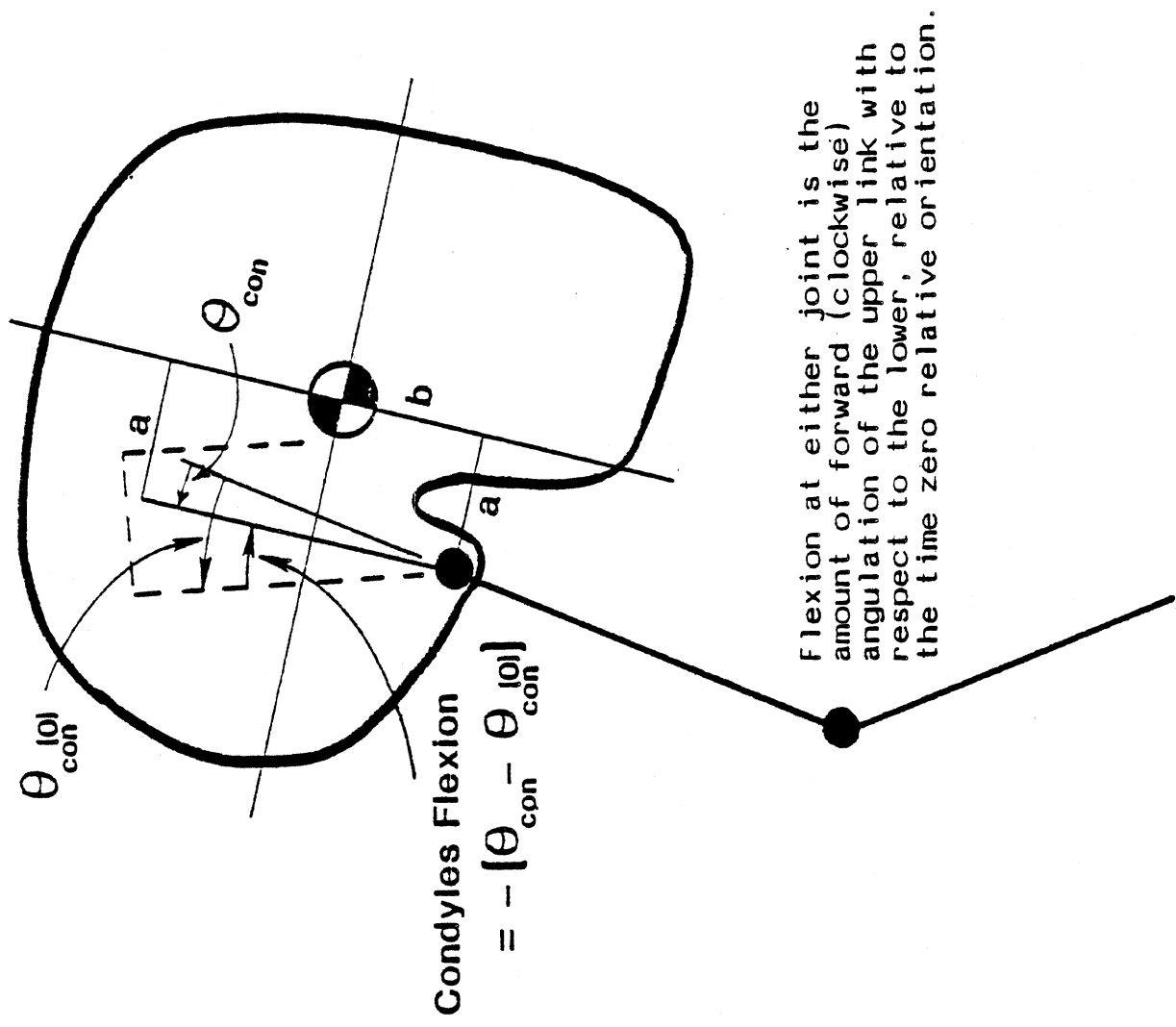
Flexion and extension at each joint are zero, by definition, at  $t=0$ .

Figure 2. C7-T1 and Condyles Angles at  $t=0$



C7 Extension  
 $= -[\theta_{C7} - \theta_{C7}^{|0|}]$

Extension at either joint is the amount of rearward (counter-clockwise) angulation of the upper link with respect to the lower, relative to the time zero relative orientation.



Condyles Flexion  
 $= -[\theta_{con} - \theta_{con}^{|0|}]$

Flexion at either joint is the amount of forward (clockwise) angulation of the upper link with respect to the lower, relative to the time zero relative orientation.

Figure 3. Definition of Extension Angle in MVMA 2-D Simulations

Figure 4. Definition of Flexion Angle in MVMA 2-D Simulations

Table 1. Test Parameters for Wayne State Sled Tests.

Test #	Test Type	Shoulder Belt	Direction of Impact	Velocity (mph)	Deceleration (g's)	Subject
DOT307	SLED	SB	FRONTAL	NA	5	Embalmed Cadaver
DOT308	SLED	SB	FRONTAL	12.0	5	Embalmed Cadaver
DOT309	SLED	NSB	FRONTAL	12.0	4	Embalmed Cadaver
DOT310	SLED	NSB	FRONTAL	22.0	22	Embalmed Cadaver
DOT314	SLED	NSB	FRONTAL	NA	25	Embalmed Cadaver
DOT331	SLED	SB	FRONTAL	NA	20	Embalmed Cadaver
DOT332	SLED	NSB	FRONTAL	NA	5	Embalmed Cadaver
DOT333	SLED	NSB	FRONTAL	NA	30	Embalmed Cadaver
DOT343	SLED	NSB	FRONTAL	NA	20	Unembalmed Cadaver
DOT345	SLED	NSB	FRONTAL	NA	10	Unembalmed Cadaver
DOT453	SLED	NSB	FRONTAL	NA	5.7	Volunteer
DOT454	SLED	NSB	FRONTAL	NA	5.7	Volunteer
DOT455	SLED	NSB	FRONTAL	NA	5.7	Volunteer

## MODELING THE WAYNE STATE DATA WITH THE MVMA 2-D SIMULATION

Several differences were noted in the test conditions of the Wayne State data that had not been encountered in previous studies of the NBDL volunteer tests.

1) The occupant restraint systems in the Wayne State tests were two-point lap belts and three-point shoulder/lap belts, as opposed to the four-point restraint used in the NBDL tests. The maximum angular rotations at T1 in the NBDL study have been about 5 degrees. In contrast, angular displacements of 35 to 55 degrees were noted in the Wayne State data. In the MVMA 2-D simulation, the torso and C7-T1 are constrained to the same angular rotations. In order to obtain an angular motion at T1 to properly model the large angular excursions of the lap-belted occupants, the time-history of the angular acceleration at T1 was included in the data deck as a forcing input.

2) All of the experimental data for T1 motion showed an initial positive x-acceleration prior to the expected negative acceleration. Although the forces acting on the impact sled were in the -x direction, the forces transferred to T1 were primarily in the +x direction. The positive acceleration appeared to be real, with the added motion of the torso in the Wayne State tests resulting in a positive acceleration at T1 in the x axis. In some instances (e.g., DOT331), however, it was found that the flexure of a target support on the seatback of the test sled contributed to an unusually high +Gx acceleration. This was corrected by computing the motion of T1-x with respect to the laboratory reference frame, which resulted in a 50% decrease in the +Gx acceleration peak for test DOT331. Two examples of the effect of the motion of the target on T1-x are shown in Figures 5-8 for DOT331 and DOT345. The same type of correction was applied to all other test data.

3) With the calculation of the x-axis motion of the head and T1 from a laboratory reference, the effect of the moving target on the seat back of the sled was corrected. In order to correctly describe the motion of the occupant independent of sled motion, the motion of the sled, described by DCXSOP, was subtracted from the motion of T1 and the head (laboratory reference).

4) The necessity of smoothing and differentiating photometric data to provide input and comparison data for the MVMA model led to many uncertainties in the consistency of the final results. One concern was whether the differentiation was accurate enough that integration of the acceleration inputs within the model would yield values of velocity and displacement for T1 that were consistent with the original film data. With

respect to the linear accelerations at T1, the integration of the input values was acceptable in all tests. For the angular acceleration at T1, integrated values of angular displacement in the simulation were consistently 10% to 50% lower than the original values of PNB02P. In general, the difference between the integrated displacement values of the model and the photo data appeared as a lag in the T1 response. The forced angular motion at T1 had a significant effect on the response of the simulation. Figures 9-12 illustrate the angular motion and acceleration at T1 for tests DOT308 and DOT332. The acceleration values of intractable tests had peak angular accelerations twice as large as tests which were sensitive to parameter variation.

Initially, it was felt that non-zero velocities and accelerations observed in the simulation at time zero were strictly effects of the method used in the smoothing and differentiation routine, i.e., they were not true values. Although the sled motion had been subtracted from the motion of the head and T1, non-zero velocities were observed for T1 in the simulation and in the experimental values at time zero. The addition of T1 velocities at time zero was included in the MVMA data for the x and z axis motion in an attempt to improve the simulation response. The observation of low values of T1 angular motion, as cited above, and the unresponsiveness of some tests to changes in the model led to the inclusion of non-zero initial velocities in the data deck.

Initial values of head angular velocity, T1 angular velocity, and neck angular velocity were also calculated. These values were very sensitive to the amount of smoothing, however, varying significantly with the number of times the data was smoothed before and after differentiation. Overall, there was little consistency between the calculated values of angular velocity at T1, the neck, and the head for each test subject. The use of initial angular velocities improved certain aspects of intractable tests (e.g., DOT332.DAT), but these simulations remained insensitive to parameter changes.

5) The location of T1 in the digitized data was subject to a certain amount of guesswork when the film analysis was performed. If T1 was positioned posteriorly of its proper location, an extension motion in excess of the experimental values could have resulted from an unduly large lever arm for moments associated with axial neck forces at the condyles. In one run (DOT345.DAT), the location of T1 was moved forward 2 cm and the initial neck length and neck angle were recalculated. The bending moment was reduced at the condyles as a result of the shift in the location of T1, but it was concluded that this had only a small effect on the overall results.

6) The location of the head center of gravity was recalculated to account for the difference between the location of the acceleration sensors in the NBDL tests and the Wayne State tests. The volunteer subjects of the NBDL tests were instrumented with an accelerometer bite-plate which shifted the

head cg forward by .35 centimeters. The Wayne State subjects were instrumented with an accelerometer pack on the crown of the head, resulting in a rearward shift in the head cg. This difference was estimated and the MVMA 2-D data were revised to reflect the change in the head cg location.

7) Small variations were noted in the calculated neck lengths in cadaver WC3788 (DOT307-DOT310) and volunteer VO2520 (DOT453-DOT455), but no corrections were made to obtain an average neck length. The calculated neck length of WC3788 varied from 13.2 to 14.6 cm. The neck length of VO2520 varied from 8.44 cm to 10.25 cm. It was apparent that the initial values of the neck angle and neck length were sensitive to smoothing as well. The time zero neck angle varied by as much as ten degrees depending on whether the values were smoothed or unsmoothed.

8) With regard to the reliability of the test data, test DOT309 had digitized time-histories which resulted in very large acceleration inputs that were unrealistic. The simulation of DOT309 was not pursued further.

## DISCUSSION

The use of photometric data to describe the head/neck response of the Wayne State test subjects was not sufficient to provide a consistent set of inputs and experimental comparison results for each test investigated. Initially, it was thought that the 200 hertz sampling rate of digitized position was insufficient to allow accurate numerical differentiation for velocities and accelerations of the test subjects. The film speed was a factor in limiting the accuracy of the differentiated time-histories, but the scatter in measured values compounded the difficulty of differentiating time-histories from a low sampling rate.

It was particularly difficult to obtain the correct angular motion at T1 from the differentiated data. In several of the tests investigated, the forcing input for T1 angular motion was inadequate to drive the head/neck model correctly. Lacking the correct forcing input, the simulations of the head/neck response were not in good agreement with the experimental results.

In future investigations, alternative methods could be devised to obtain T1 angular acceleration in the model. If sensor data were not available for the derivation of T1 angular motion, a fixed linkage for the torso could be defined such that the linear resultant acceleration at T1 would serve as the forcing excitation for the angular motion of the torso.

### Simulation Results

The sensitivity of the simulation to parameter variation was evaluated on the size of parameter values necessary to change the response of the simulation. Differentiated test data were viewed as intractable for modeling purposes if stiffnesses and damping coefficients 2 to 3 times greater than the NBDL data resulted in little or no change in the simulation. In this sense, DOT331, DOT332, and DOT345 were largely insensitive to changes in the model parameters. The three volunteer tests DOT453, DOT454, and DOT455, and one cadaver test, DOT308, however, displayed sufficient sensitivity to the model parameters to allow a limited parameter variation study.

The values of MVMA 2-D model parameters initially used in the present study were developed from earlier simulations of the head/neck response of Navy volunteer test subjects (1). The model parameter values that produced the best match to sagittal plane motion of the NBDL tests are shown in Table 2.



Table 2. HEAD-NECK BIOMECHANICAL PARAMETER VALUES  
DETERMINED IN NBDL SIMULATIONS

	Preliminary Value
At Neck-Head Articulation (condyles)	
Flexion Bending Stiffness	2.5 N-m/deg
Flexion Damping Coefficient in Loading	.026 N-m-s/deg
Flexion Damping Coefficient in Unloading	.026 N-m-s/deg
Flexion Energy Restitution Coefficient	.5
Extension Bending Stiffness	.714 N-m/deg
Extension Damping Coefficient in Loading	0. N-m-s/deg
Extension Damping Coefficient in Unloading	.026 N-m-s/deg
Extension Energy Restitution Coefficient	.95
At Neck-Torso Articulation (C7/T1)	
Flexion Bending Stiffness	1.6 N-m/deg
Flexion Damping Coefficient in Loading	0. N-m-s/deg
Flexion Damping Coefficient in Unloading	0. N-m-s/deg
Flexion Energy Restitution Coefficient	.11
Extension Bending Stiffness	.457 Nm/deg
Extension Damping Coefficient in Loading	0. N-m-s/deg
Extension Damping Coefficient in Unloading	0. N-m-s/deg
Extension Energy Restitution Coefficient	.10
For Axial Neck Elongation and Compression	
Elongation Stiffness	1644 N/cm
Elongation Damping Coefficient in Loading	15.0 N-s/cm
Elongation Damping Coefficient in Unloading	15.0 N-s/cm
Elongation Energy Restitution Coefficient	.99
Compression Stiffness	400 N/cm
Compression Damping Coefficient in Loading	15.0 N-s/cm
Compression Damping Coefficient in Unloading	15.0 N-s/cm
Compression Energy Restitution Coefficient	.99

The initial simulations of the Wayne State data were carried out with the NBDL model parameters shown in Table 2, but it was necessary to increase the values of the stiffness at C7 and the condyles. Earlier, a ratio of flexion stiffness to extension stiffness of 3.5 was used at the condyles and C7, based on the data of Mertz and Patrick (3). An accurate value could not be established from the simulation of NBDL volunteer tests because the tests did not produce an appreciable extension at either the condyles or C7/T1 and thus did not test the values of extension stiffness. In the volunteer tests, the ratio of flexion to extension stiffness was decreased at C7 to approximately 3.0, due to larger extension stiffnesses. In the case of DOT308, an embalmed cadaver test subject, a ratio of .8 was used at C7 and the condyles.

Of the tests analyzed in the present study, the Wayne State volunteer tests DOT454 and DOT455 gave the most reliable indication of the values of stiffness and damping for extension. In Table 3, the values for the neck-head articulation and the neck-torso articulation are given for these two tests. Although the simulations were not very good and the parameter values are only approximate, they provide some measure of stiffness and damping for extension observed for the volunteer subjects.

The results of the adjusted model parameters for test DOT308, an embalmed cadaver subject restrained in a three-point lap/shoulder belt, are shown in figures 13 through 21 for the time-histories of the forcing inputs and the response variables. The values of the model parameters for neck-head articulation and neck-torso articulation are given in Table 4. A primary difficulty in modeling the response of DOT308 was an inconsistency of experimental T1 angular position, velocity, and acceleration data. An effect of this is shown in the lag in the head angular motion observed in Figure 15, which was accompanied by a lagged angular motion at the torso and T1 in the simulation. No further variation in the model parameters could improve the response for the head motion shown in Figures 15-17.

The Wayne State volunteer test results for DOT453 are shown in Figures 21-30, DOT454 results are shown in Figures 31-39, and DOT455 results are shown in Figures 40-48. The adjusted MVMA 2-D model parameters of Table 3 had the "best" fit for test DOT455. DOT453 and DOT454 displayed good agreement in the extension motion of the head, but a large overshoot in the forward angular motion subsequently occurred. In an attempt to decrease the overshoot in the head angular motion, the flexion stiffness at the condyles was increased in DOT454. The comparison of the first and second adjustment of the model parameters of DOT454 are shown in Figures 49-60. A large increase in the flexion stiffness at the condyles had only a small effect on DOT454; the overshoot was present in the head angle to a lesser degree and a closer agreement in the rebound of the head velocity was observed (Figure 52).

Table 3. HEAD-NECK BIOMECHANICAL PARAMETER VALUES  
DETERMINED FOR WAYNE STATE VOLUNTEERS.

	Preliminary Value
At Neck-Head Articulation (condyles)	
Flexion Bending Stiffness	2.5 N-m/deg
Flexion Damping Coefficient in Loading	.026 N-m-s/deg
Flexion Damping Coefficient in Unloading	.026 N-m-s/deg
Flexion Energy Restitution Coefficient	.5
Extension Bending Stiffness	.714 N-m/deg
Extension Damping Coefficient in Loading	.026 N-m-s/deg
Extension Damping Coefficient in Unloading	.026 N-m-s/deg
Extension Energy Restitution Coefficient	.95
At Neck-Torso Articulation (C7/T1)	
Flexion Bending Stiffness	2.4 N-m/deg
Flexion Damping Coefficient in Loading	.0262 N-m-s/deg
Flexion Damping Coefficient in Unloading	.026 N-m-s/deg
Flexion Energy Restitution Coefficient	.11
Extension Bending Stiffness	.840 Nm/deg
Extension Damping Coefficient in Loading	.0034 N-m-s/deg
Extension Damping Coefficient in Unloading	.0034 N-m-s/deg
Extension Energy Restitution Coefficient	.10
For Axial Neck Elongation and Compression	
Elongation Stiffness	1644 N/cm
Elongation Damping Coefficient in Loading	15.0 N-s/cm
Elongation Damping Coefficient in Unloading	15.0 N-s/cm
Elongation Energy Restitution Coefficient	.99
Compression Stiffness	400 N/cm
Compression Damping Coefficient in Loading	15.0 N-s/cm
Compression Damping Coefficient in Unloading	15.0 N-s/cm
Compression Energy Restitution Coefficient	.99

Table 4. HEAD-NECK BIOMECHANICAL PARAMETER VALUES  
 DETERMINED FOR WAYNE STATE CADAVER TEST  
 DOT308.

	Preliminary Value
At Neck-Head Articulation (condyles)	
Flexion Bending Stiffness	2.5 N-m/deg
Flexion Damping Coefficient in Loading	.026 N-m-s/deg
Flexion Damping Coefficient in Unloading	.026 N-m-s/deg
Flexion Energy Restitution Coefficient	.5
Extension Bending Stiffness	3.12 N-m/deg
Extension Damping Coefficient in Loading	.026 N-m-s/deg
Extension Damping Coefficient in Unloading	.026 N-m-s/deg
Extension Energy Restitution Coefficient	.95
At Neck-Torso Articulation (C7/T1)	
Flexion Bending Stiffness	1.6 N-m/deg
Flexion Damping Coefficient in Loading	0. N-m-s/deg
Flexion Damping Coefficient in Unloading	0. N-m-s/deg
Flexion Energy Restitution Coefficient	.11
Extension Bending Stiffness	2.0 Nm/deg
Extension Damping Coefficient in Loading	.0034 N-m-s/deg
Extension Damping Coefficient in Unloading	.0034 N-m-s/deg
Extension Energy Restitution Coefficient	.10
For Axial Neck Elongation and Compression	
Elongation Stiffness	1644 N/cm
Elongation Damping Coefficient in Loading	15.0 N-s/cm
Elongation Damping Coefficient in Unloading	15.0 N-s/cm
Elongation Energy Restitution Coefficient	.99
Compression Stiffness	400 N/cm
Compression Damping Coefficient in Loading	15.0 N-s/cm
Compression Damping Coefficient in Unloading	15.0 N-s/cm
Compression Energy Restitution Coefficient	.99

Modeling the Wayne State test subjects with values of stiffness and damping coefficients in extension and flexion that greatly exceeded the constants specified in Tables 3 and 4 resulted in only minor improvements in the agreement between simulation results and the experimental data for DOT308, and DOT453-DOT455. It did not appear that any additional information would be gained by using significantly larger parameter values in the simulation to marginally improve the simulation results. Such large values would compromise the simulation of head/neck dynamic response if they were retained in the model.

One observation was drawn from the cross plot of head angle versus neck angle for the Wayne State data. The tests which displayed sensitivity to changes in the model parameters appeared to have a characteristic signature that other, less tractable simulations did not possess. The general observation of an initial extension followed by a long period of forward motion by the head and neck appeared characteristic for the four tests that were sensitive to parameter variation. In Figures 61-66, examples of head/neck angles are shown for the simulations of DOT331, DOT345, DOT308, DOT453, DOT454, and DOT455. It should be noted, however, that the plots of head versus neck angle in Figures 61-66 are from the MVMA simulation and may not reflect the true motion of the test subjects. The plots for tests DOT308 and DOT455 are close to the experimental data for the head/neck angle, but the other plots are less representative of the actual motion.

The long duration of a combined forward motion of the head and neck in Figures 63-66 was of interest in regard to the amount of articulation at the condyles after the initial extension. Earlier, it had been observed in the NBDL tests that the condyles could become locked during the impact event, altering the conditions under which a test was simulated (4,5). In the event of locked condyles, the head/neck cross plot would show the head and neck angles changing at a constant rate with respect to the laboratory reference. In addition, the expected slope of head angle versus neck angle would be unity. The head and neck did change largely at a constant rate in the simulation of test DOT455 (Figure 66), for example, but the slope of head angle versus neck angle was not unity. The observed slope had a value of approximately two, indicating that the head angular position changed at a rate two times the rate of neck angular motion. In Figures 63-66, the angular rate of change of the head relative to the neck was greater than one in each test, suggesting that the condyles were not locked in tests DOT308, DOT453, DOT454, and DOT455.

It was suggested that the amount of motion at T1 allowed by the different restraint systems used in the Wayne State and NBDL tests resulted in the observed differences of the angular motion of the head and neck (6). The four-point restraint used in the NBDL tests allowed a maximum rotation of five degrees at T1 and the ratio of head/neck angular motion was 1. The three-point restraint, e.g., DOT331, allowed a maximum rotation of eleven

degrees at T1 and the ratio of head/neck motion was 1.4. With a two-point restraint, e.g., DOT455, the angular rotation at T1 was forty-five degrees and the ratio of head/neck motion was approximately 2. These results would indicate that the articulation at C7/T1 relative to the condyles was dependent on the type of restraint system used in the impact test.

It is interesting to note that a comparison of the angulation of the head relative to the torso for the NBDL 6 g "averaged" tests (1) versus the volunteer test DOT455 showed a maximum motion of 45 degrees for both.

#### Summary of Objectives

The objectives of this study, as outlined earlier, were to compare the biomechanical properties and response characteristics for various test parameters described in Table 1. The parameters of interest were: 1) volunteer subjects versus cadaver subjects, 2) embalmed versus unembalmed cadavers, 3) the two-point restraint versus the three-point restraint, and 4) "tense" versus "relaxed" volunteer test subjects. To the extent that it was possible, each question was addressed by comparing simulation results for tests which differed only in the test parameters of interest.

1. Volunteer vs. Cadaver Subjects. The comparison of the model parameters of the cadaver test DOT308 to the three volunteer tests is limited due to the poor agreement in the simulation results. It does appear, however, that the embalmed cadaver displayed biomechanical properties that suggested a greater resistance to extension at the condyles than the volunteer test subjects. Drawing upon the experimental data for the maximum excursions of the head and T1 in extension and flexion, the volunteers demonstrated larger excursions in extension than either the embalmed or the unembalmed cadavers. The largest excursions in flexion, however, were observed for the unembalmed cadaver.

2. Embalmed vs. Unembalmed Cadavers. A comparison of the experimental values of maximum angular excursions of the head and T1 of embalmed and unembalmed cadavers indicated that the embalmed cadaver displayed less articulation at both the condyles and C7/T1. The maximum excursion of an embalmed cadaver in test DOT332 was fifty-four degrees for T1 and eighty-six degrees for the head. The excursions of T1 and the head for two unembalmed cadavers, DOT343 and DOT345 were twenty to twenty-five degrees greater at T1, and ten to twenty degrees greater for the head. Modeling of the biomechanical properties of the head and neck of the cadaver test subjects may indicate larger stiffnesses at the condyles and C7/T1 in the embalmed cadaver, but there were no successful simulations of cadaver test subjects in the two-point restraint to verify this assumption.

3. Two-Point vs. Three-Point Restraint. The effect of the two types of occupant restraints on the motion of test subjects was distinguished by the degree of angular rotation at T1 and the torso. The earlier discussion of the effect of the four-point restraint of the NBDL tests versus the three-point and two-point restraints of the Wayne State data suggested a relation between T1 motion and the relative head/neck motion. In addition to the varying degrees of head/neck motion for different restraints, a significant extension was observed in the subjects of the Wayne State sled tests that had not been previously observed in NBDL tests. The use of the two-point and three-point restraints (versus the four-point restraint) led to larger estimates of the extension stiffness at C7/T1 for the volunteer and cadaver test subjects. The present results, however, do not distinguish the influence of the two and three-point restraint on the biomechanical properties of the head and neck.

4. Tensed vs. Relaxed Subjects. The volunteer tests DOT453 and DOT454 were similar in many respects. The data of the MVMA simulation summarized in Table 3 best fit test DOT455, while DOT453 and DOT454 were not quite as close in agreement. The tense versus relaxed pattern among the volunteer tests designated tests DOT453 and DOT455 as the "tensed" test subjects and DOT454 was the "relaxed" test subject. This particular pattern was not evidenced in any way in the modeling and simulation results, however.

## RECOMMENDATIONS

The use of response data from different dynamic test conditions creates the possibility for evaluating the MVMA 2-D model parameters under new conditions. For the Wayne State sled impact tests, it was possible to evaluate the extension stiffness values of the NBDL data. An estimate of the values of extension stiffness had not previously been possible from the NBDL data. It should be emphasized, however, that more reliable estimates of the extension stiffness values should be obtained.

Dr. Curt Spenny had discussed the possibility of reanalyzing the film data obtained from the Wayne State tests. If this is done, it is recommended that particular attention be devoted to the measurement of T1 angular motion (PNB02P). A frame rate of 1000 frames per second is recommended in future tests. The entire duration of the impact event should be digitized as well.

The success of using photometric data in the investigation of head/neck dynamics is strongly dependent on the fidelity of the numerical differentiation and smoothing. For future studies of this kind, it is recommended that a portion of the work be devoted to the development of numerical differentiation and smoothing routines that are able to provide consistent estimates of velocity and acceleration.

Finally, it is strongly recommended that sensor data be used along with photometric data when these data are available for the analysis of either the kinematics or the dynamics of the head and neck. Further, all experimental test programs should include the collection of sensor data since photometric data alone have been demonstrated to be of limited value.



## LITERATURE CITED

1. Schneider, L.W., and Bowman, B.M., "Prediction of Head/Neck Dynamic Response of Selected Military Subjects to -Gx Acceleration." Proceedings of Symposium on Biodynamic Models, Dayton, February 1977, Aviation, Space, and Environmental Medicine, pp. 211-223, Vol. 49, No. 1, January, 1978.
2. Bowman, B.M., Schneider, L.W., Lustick, L.S., Anderson, W.R., and Thomas, D.J., "Simulation Analysis of Head and Neck Dynamic Response." Proceedings, Twenty-Eighth Stapp Car Crash Conference. Society of Automotive Engineers Inc., Warrendale, PA, SAE #841668, November 1984.
3. Mertz, H.J., and Patrick, L.M., "Strength and Response of the Human Neck." Proceedings, Fifteenth Stapp Car Crash Conference. Society of Automotive Engineers Inc., Warrendale, PA, SAE #710855, November 1971.
4. Seeman, M.R., Lustick, L.S., Frisch, G.D., "Mechanism for Control of Head and Neck Dynamic Response." Proceedings, Twenty-Eighth Stapp Car Crash Conference. Society of Automotive Engineers Inc., Warrendale, PA, SAE #841669, 1984.
5. Wismans, J., Spenny, C. H., "Head-Neck Response in Frontal Flexion." Proceedings, Twenty-Eighth Stapp Car Crash Conference. Society of Automotive Engineers Inc., Warrendale, PA, SAE #841666, 1984.
6. Personal communication C. H. Spenny.

J-11 X-ACCELERATION  
 MAYNE STATE DOT 331 -GX AT 20 G'S  
 T1 MOTION FORCED

M=2.5; T1IF=5.33; E=55.0; GZ/NIF=1.6; 0+0..11  
 PHOTOELECTRIC DATA FOR SUBJECT KC3946

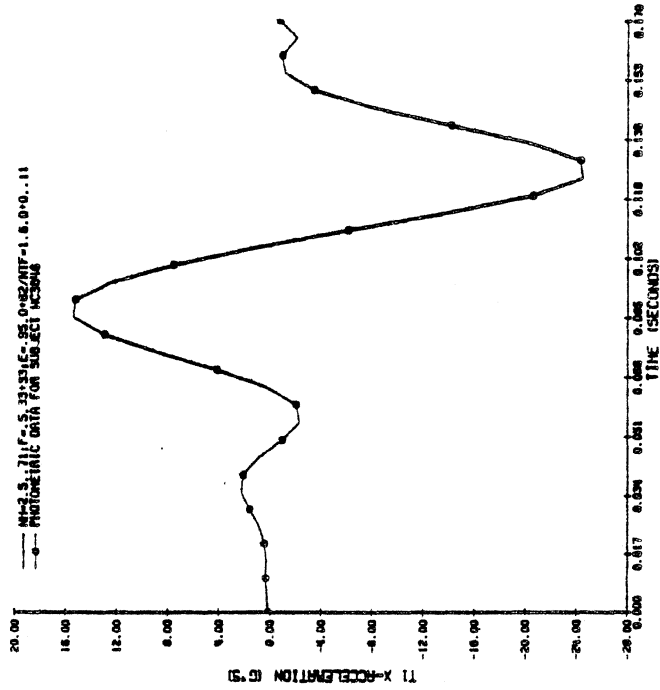


FIGURE 5. UNCORRECTED T1 X-ACCELERATION DOT331.

J-11 X-ACCELERATION  
 MAYNE STATE DOT 331 -GX AT 20 G'S  
 T1 MOTION FORCED

M=2.5; T1IF=5.33; E=55.0; GZ/NIF=1.6; 0+0..11  
 PHOTOELECTRIC DATA FOR SUBJECT KC3946

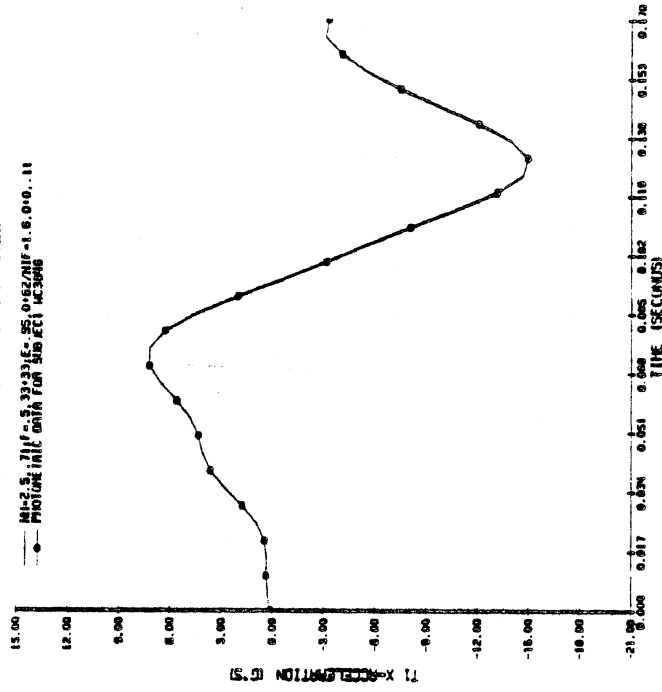


FIGURE 6. CORRECTED T1 X-ACCELERATION DOT331.

1-11 X-ACCELERATION  
 WAYNE STATE DOT 345 -GX AT 10 G'S  
 11 MOTION FORCED

MI-2.5.711F-5.3213E-25.0152/MIF-1.6.0+0..11  
 PHOTOELECTRIC DATA FOR SUBJECT M25938

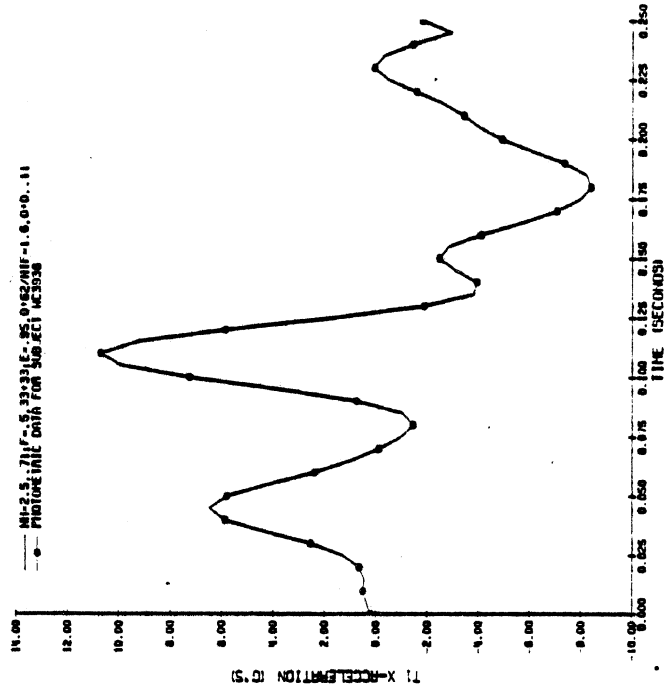


FIGURE 7. UNCORRECTED T1 X-ACCELERATION DOT345.

1-11 X-ACCELERATION  
 WAYNE STATE DOT 345 -GX AT 10 G'S  
 11 MOTION FORCED

MI-2.5.711F-5.3213E-25.0152/MIF-1.6.0+0..11  
 PHOTOELECTRIC DATA FOR SUBJECT M25938

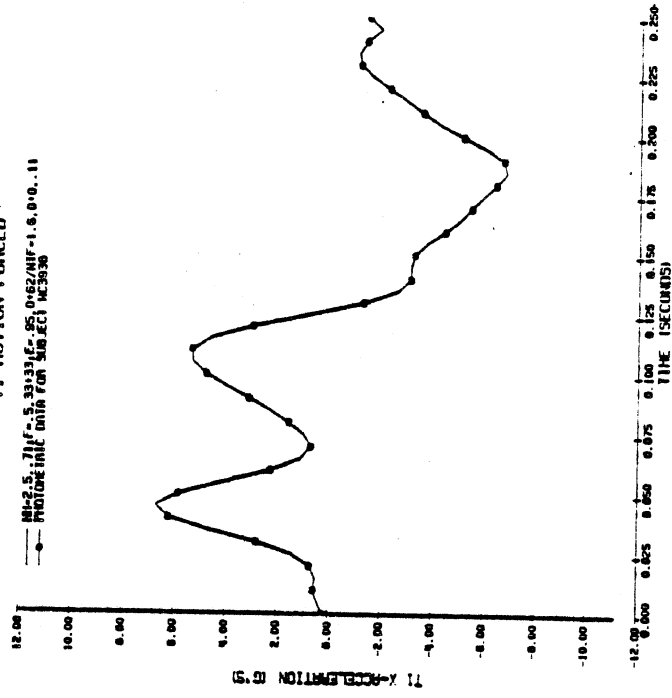


FIGURE 8. CORRECTED T1 X-ACCELERATION DOT345.

T1 ANGULAR POSITION  
WAYNE STATE DOT.308, -GX AT 5 G'S

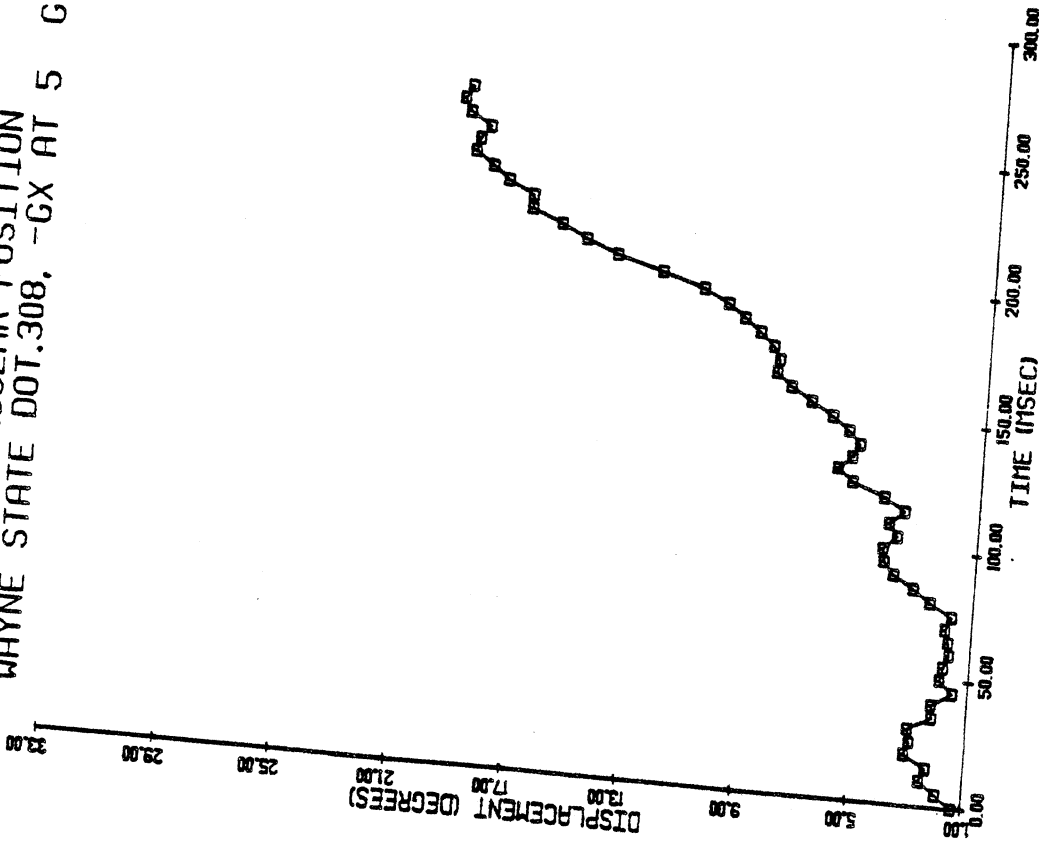


FIGURE 9. T1 ANGULAR POSITION (PNB02P) DOT308.

T1 ANGULAR ACCELERATION  
WAYNE STATE DOT.308, -GX AT 5 G'S

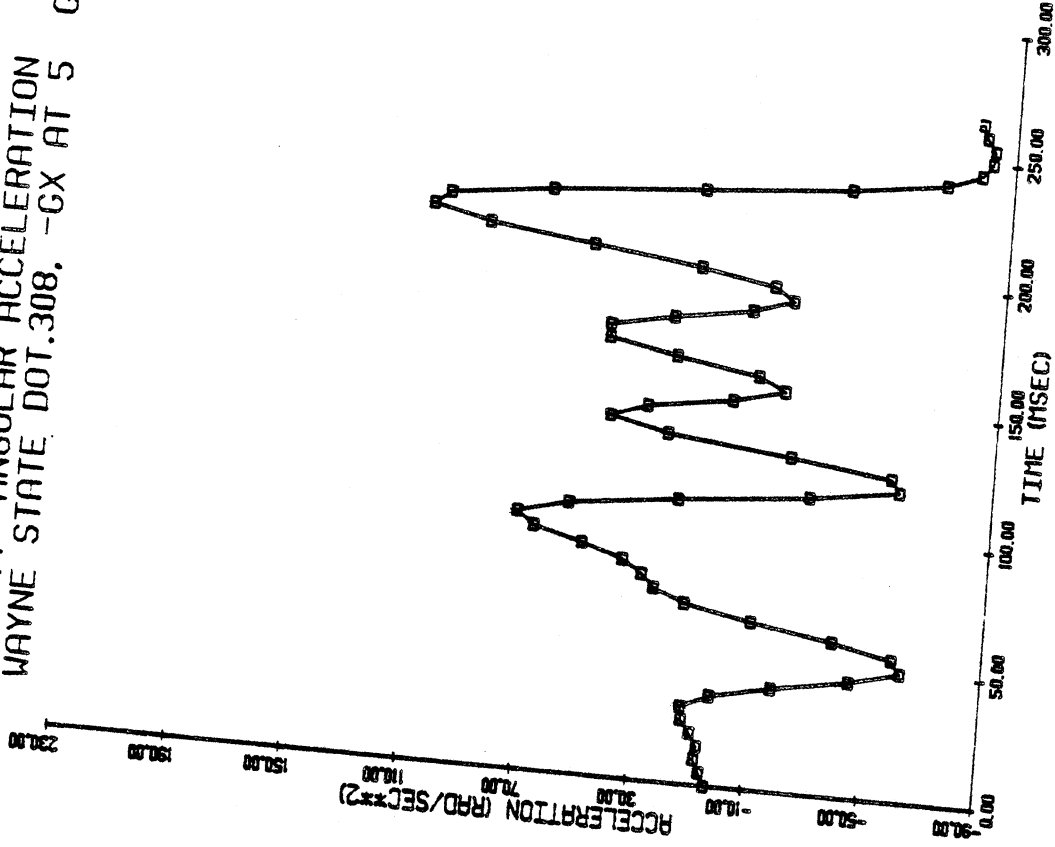


FIGURE 10. T1 ANGULAR ACCELERATION DOT308.

T1 ANGULAR POSITION  
WAYNE STATE DOT.332, -GX AT 5 G'S

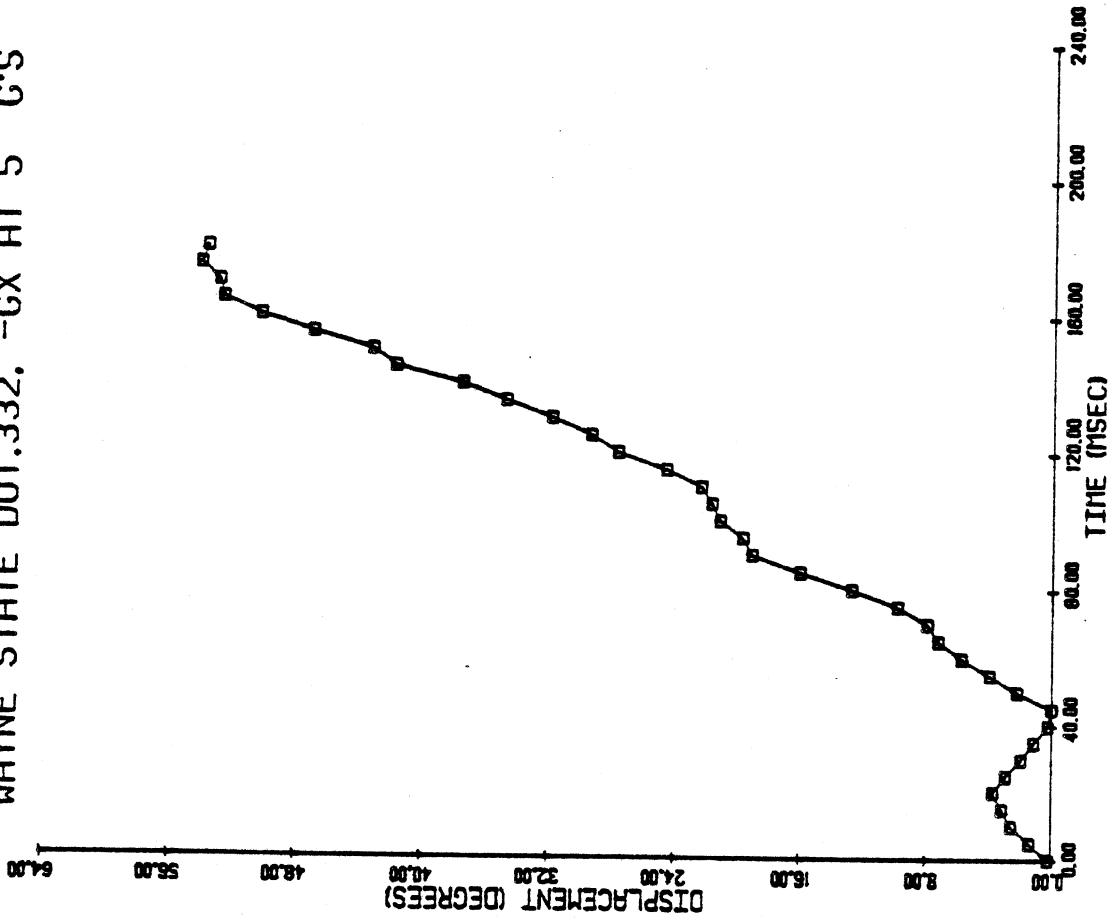


FIGURE 11. T1 ANGULAR POSITION (PNB02P) DOT332.

T1 ANGULAR ACCELERATION  
WAYNE STATE DOT.332, -GX AT 5 G'S

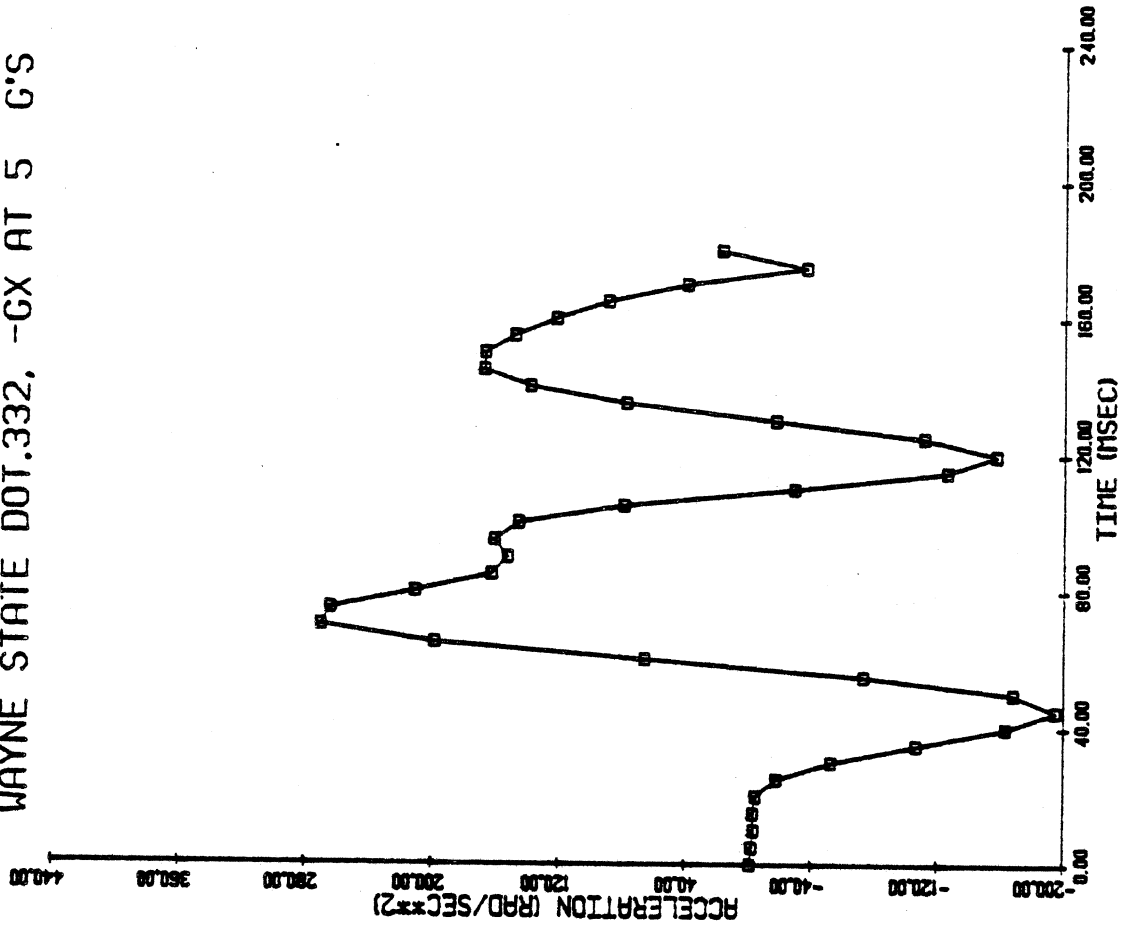


FIGURE 12. T1 ANGULAR ACCELERATION DOT332.

1-II X-ACCELERATION  
 WAYNE STATE DOT.308, -GX AT 5 G'S  
 T1 MOTION FORCED

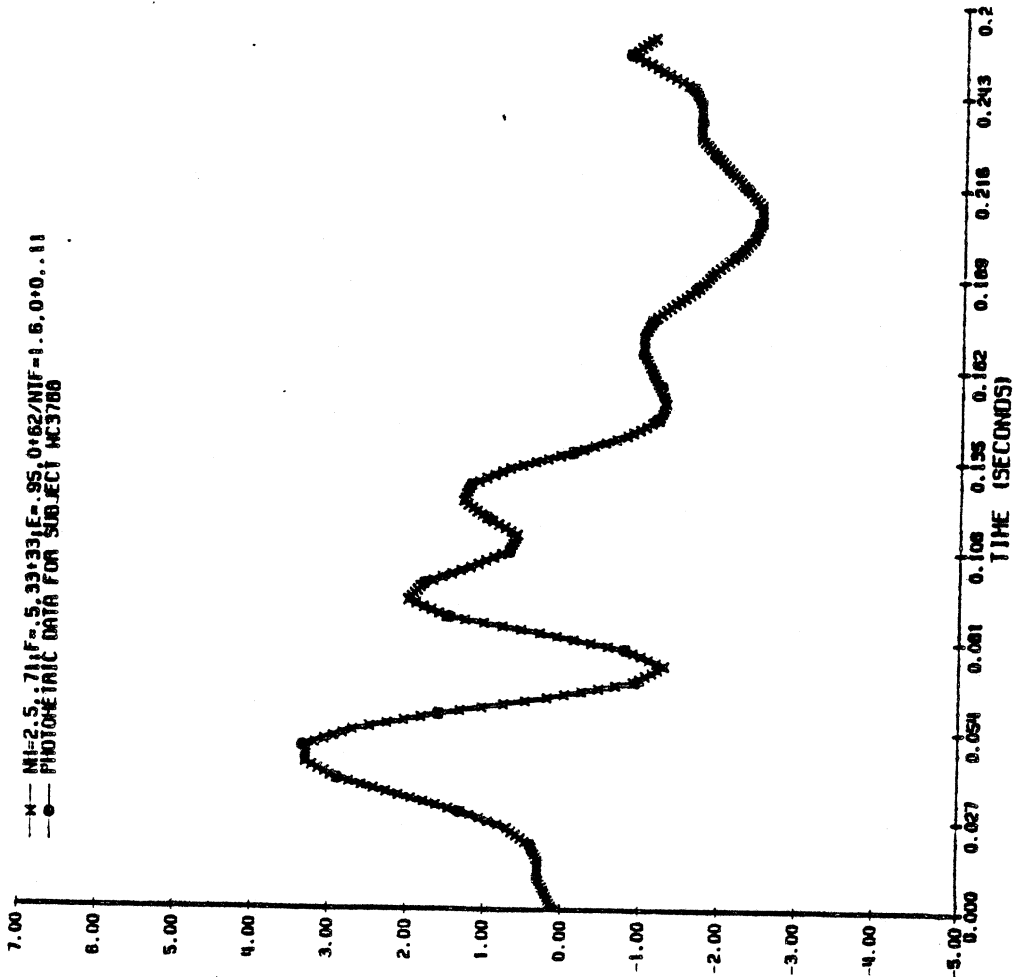


FIGURE 13. T1 X-ACCELERATION DOT308.

2-II Z-ACCELERATION  
 WAYNE STATE DOT.308, -GX AT 5 G'S  
 T1 MOTION FORCED

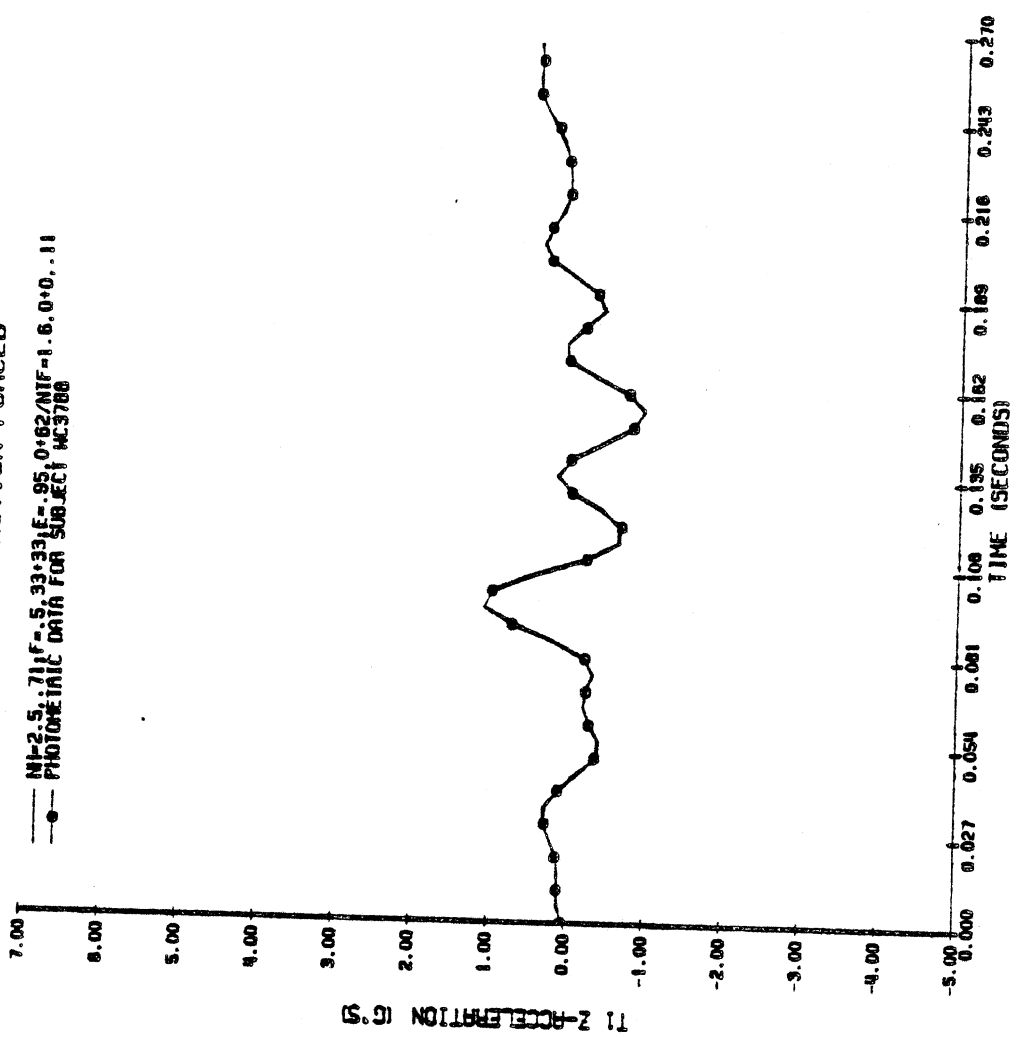


FIGURE 14. T1 Z-ACCELERATION DOT308.

3-HEAD ANGULAR POSITION  
 WAYNE STATE DOT.308, -GX AT 5 G'S  
 T1 MOTION FORCED

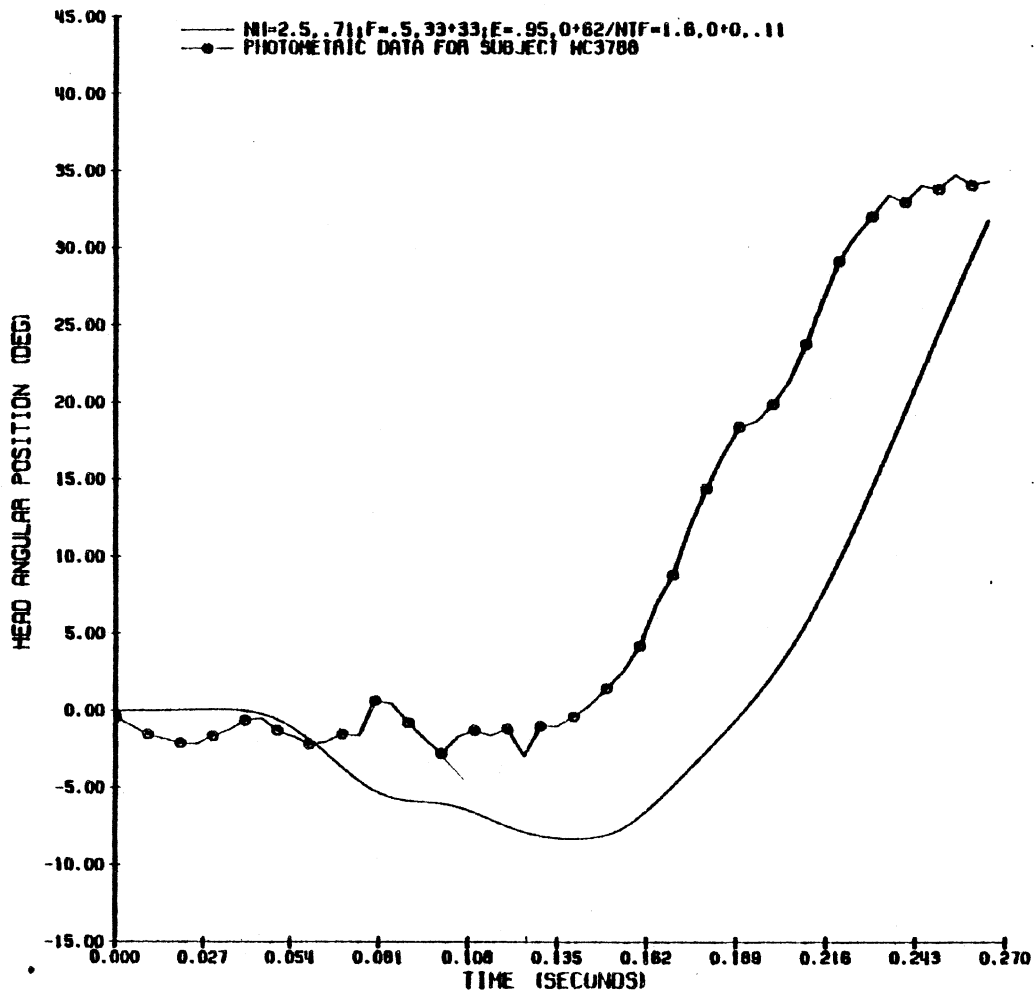


FIGURE 15. HEAD ANGULAR POSITION FOR NBDL ADJUSTED PARAMETERS DOT308.

4-HEAD ANGULAR VELOCITY  
 WAYNE STATE DOT.308, -GX AT 5 G'S  
 T1 MOTION FORCED

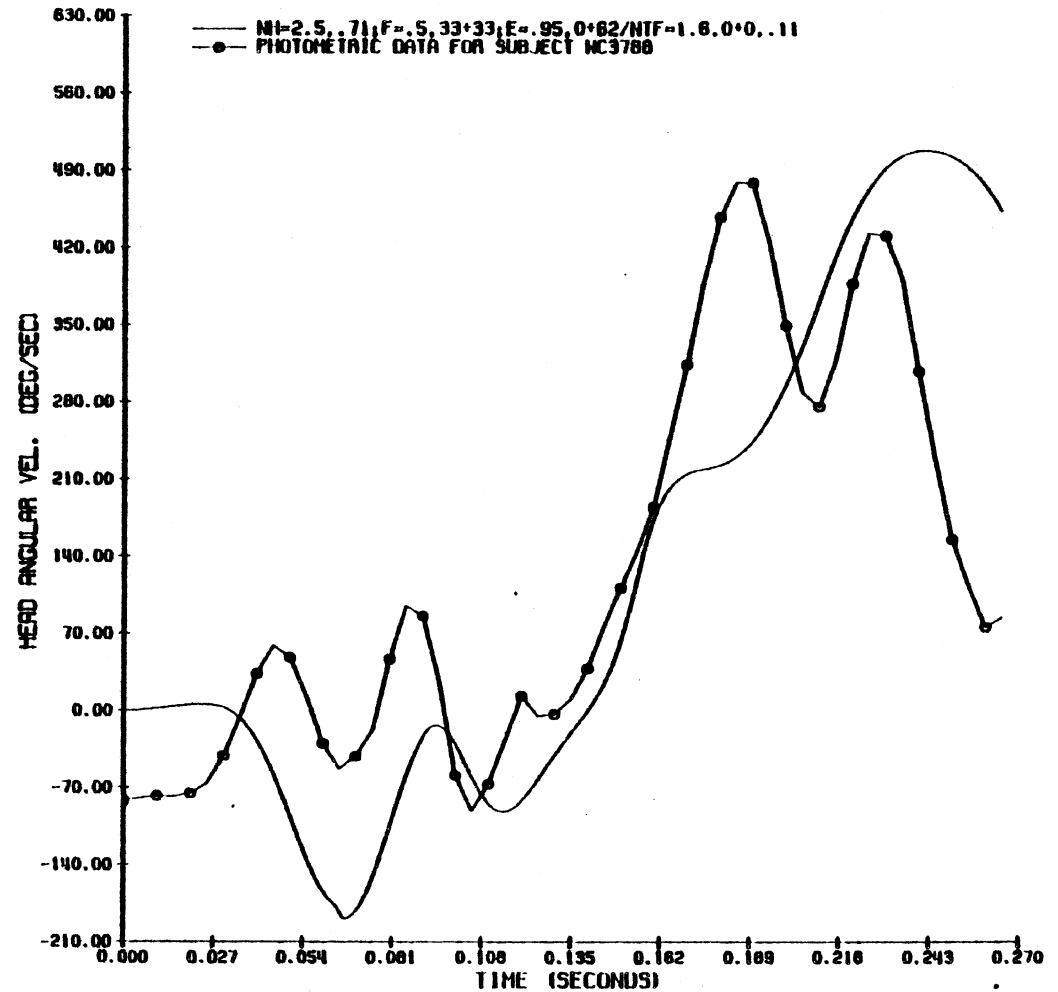


FIGURE 16. HEAD ANGULAR VELOCITY FOR NBDL ADJUSTED PARAMETERS DOT308.

5-HEAD ANGULAR ACCELERATION  
WAYNE STATE DOT 308 -GX AT 5 G'S  
11 MOTION FORCED

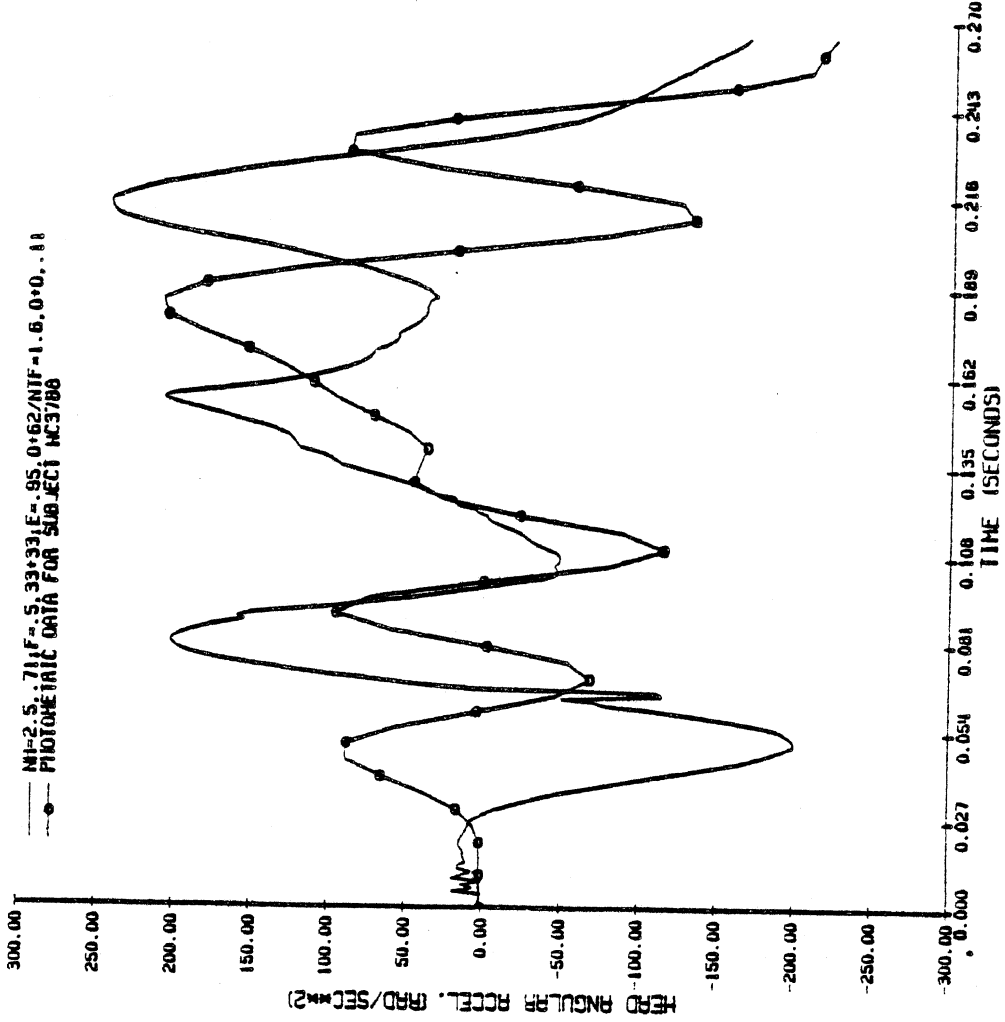


FIGURE 17. HEAD ANGULAR ACCELERATION FOR NBDL ADJUSTED PARAMETERS DOT308.

6-RESULTANT LINEAR ACCEL. OF HEAD ANATOMICAL ORIGIN  
WAYNE STATE DOT 308 -GX AT 5 G'S  
11 MOTION FORCED

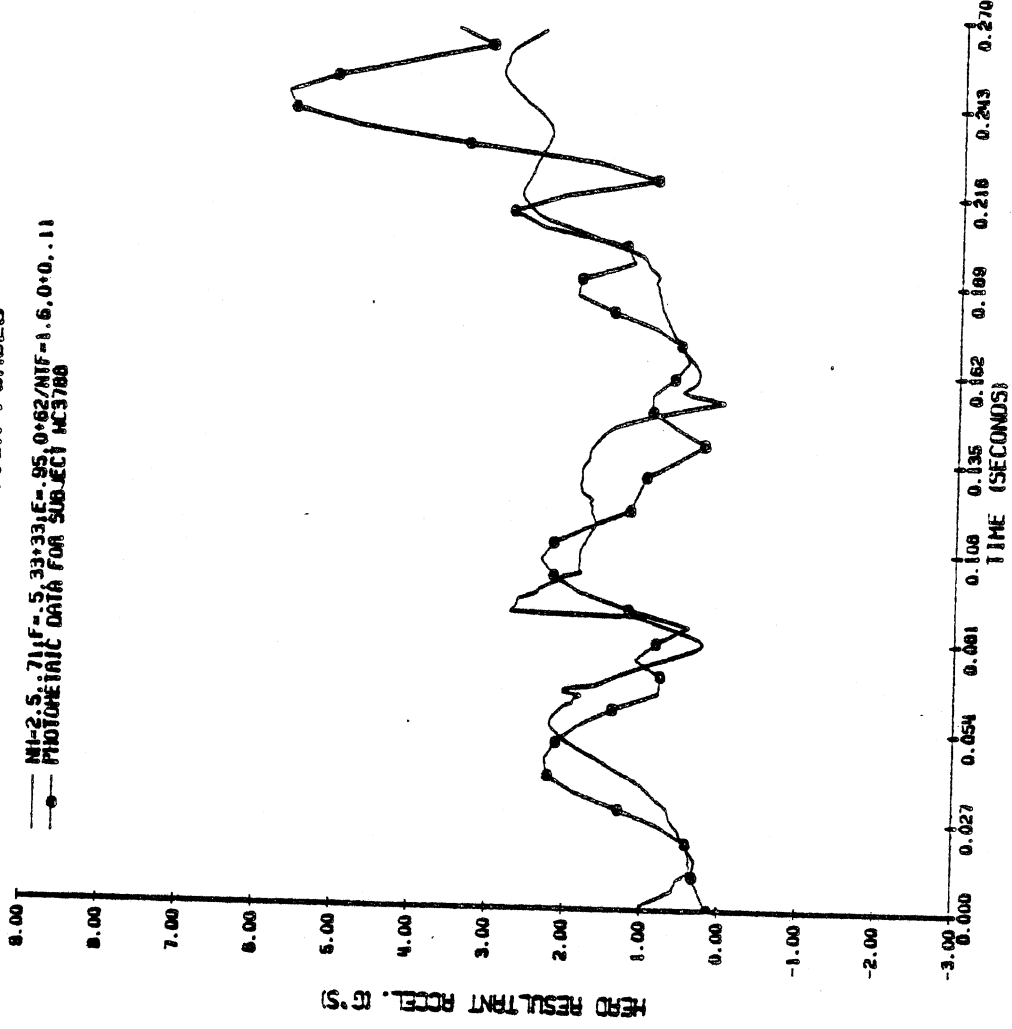


FIGURE 18. RESULTANT LINEAR ACCELERATION OF HEAD FOR NBDL ADJUSTED PARAMETERS DOT308.



19-UPPER NECK MOMENT VS. ANGLE  
WAYNE STATE DOT.308, -GX AT 5 G'S  
T1 MOTION FORCED

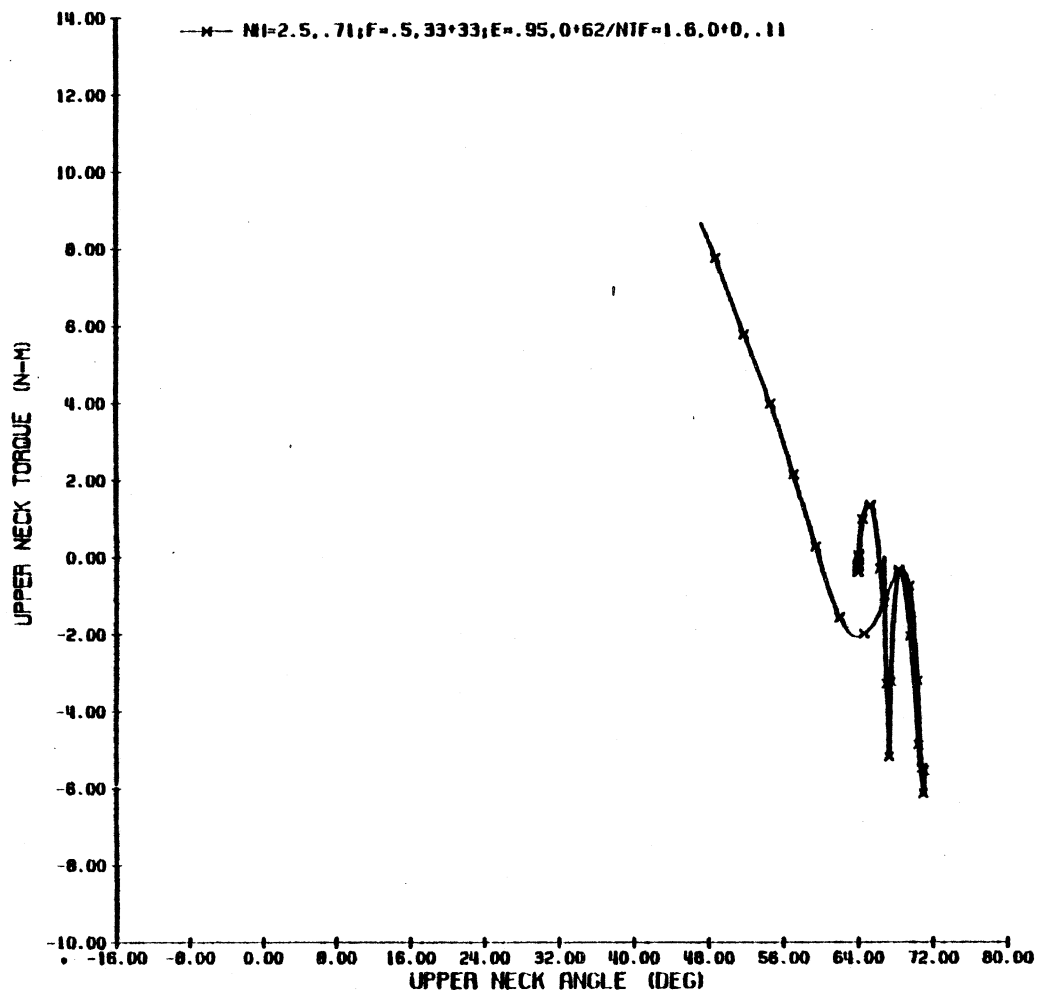


FIGURE 19. UPPER NECK MOMENT VS. NECK ANGLE FOR NBDL ADJUSTED PARAMETERS DOT308.

20-LOWER NECK MOMENT VS. ANGLE  
WAYNE STATE DOT.308, -GX AT 5 G'S  
T1 MOTION FORCED

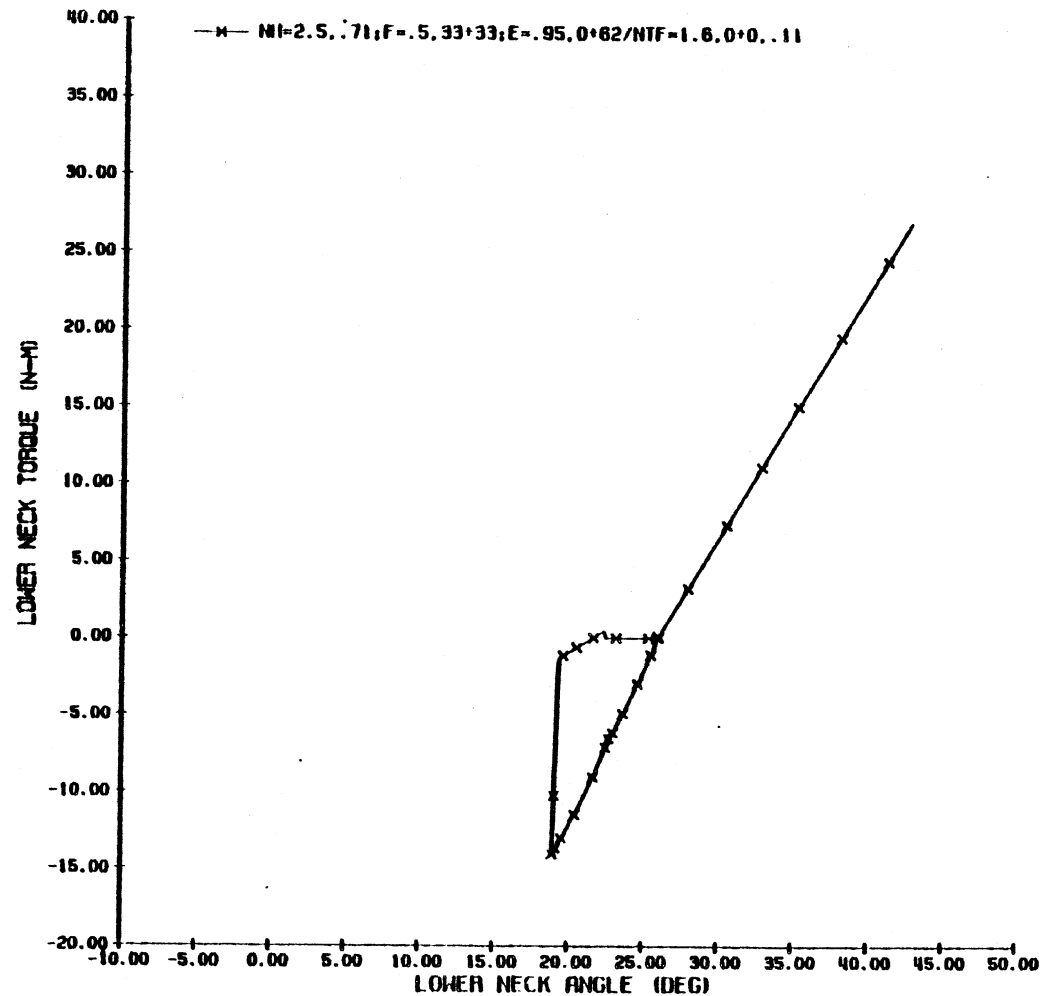


FIGURE 20. LOWER NECK MOMENT VS. NECK ANGLE FOR NBDL ADJUSTED PARAMETERS DOT308.

21-HEAD ANGLE VS. NECK ANGLE  
 WAYNE STATE DOT.308, -GX AT 5 G'S  
 TI MOTION FORCED

\* NI=2.5..71;F=-.5.33\*33;E=.95.0162/NIF-1.6.0\*0..11

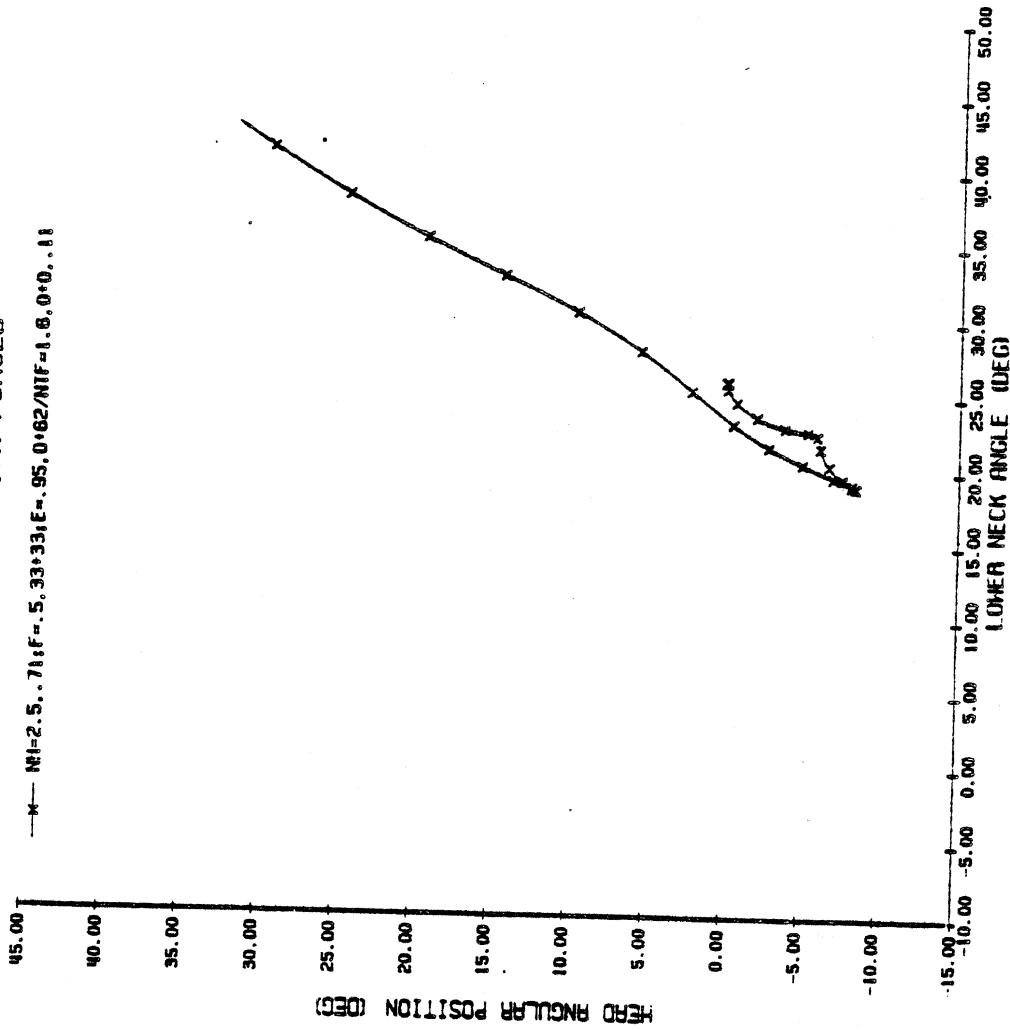


FIGURE 21. HEAD ANGLE VS. NECK ANGLE FOR NBDL ADJUSTED  
 PARAMETERS DOT308.

1-T1 X-ACCELERATION  
 WAYNE STATE DOT. 453, -GX AT 5 G'S  
 T1 MOTION FORCED

MI-2.5.71F-5.33+33IE-95.0+62/NIF-1.6.0+0.11  
 PHOTOELECTRIC DATA FOR SUBJECT WVD2520

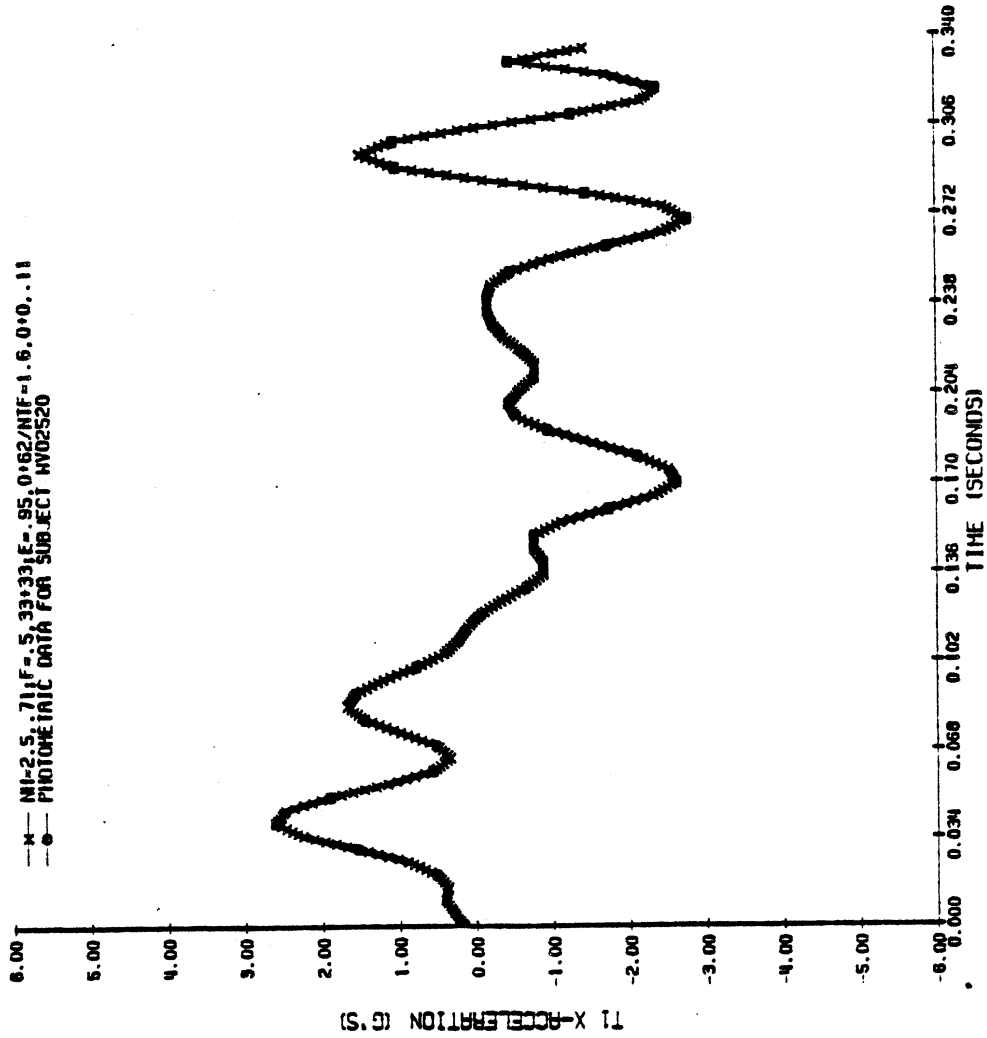


FIGURE 22. T1 X-ACCELERATION DOT453.

2-T1 Z-ACCELERATION  
 WAYNE STATE DOT. 453, -GX AT 5 G'S  
 T1 MOTION FORCED

MI-2.5.71F-5.33+33IE-95.0+62/NIF-1.6.0+0.11  
 PHOTOELECTRIC DATA FOR SUBJECT WVD2520

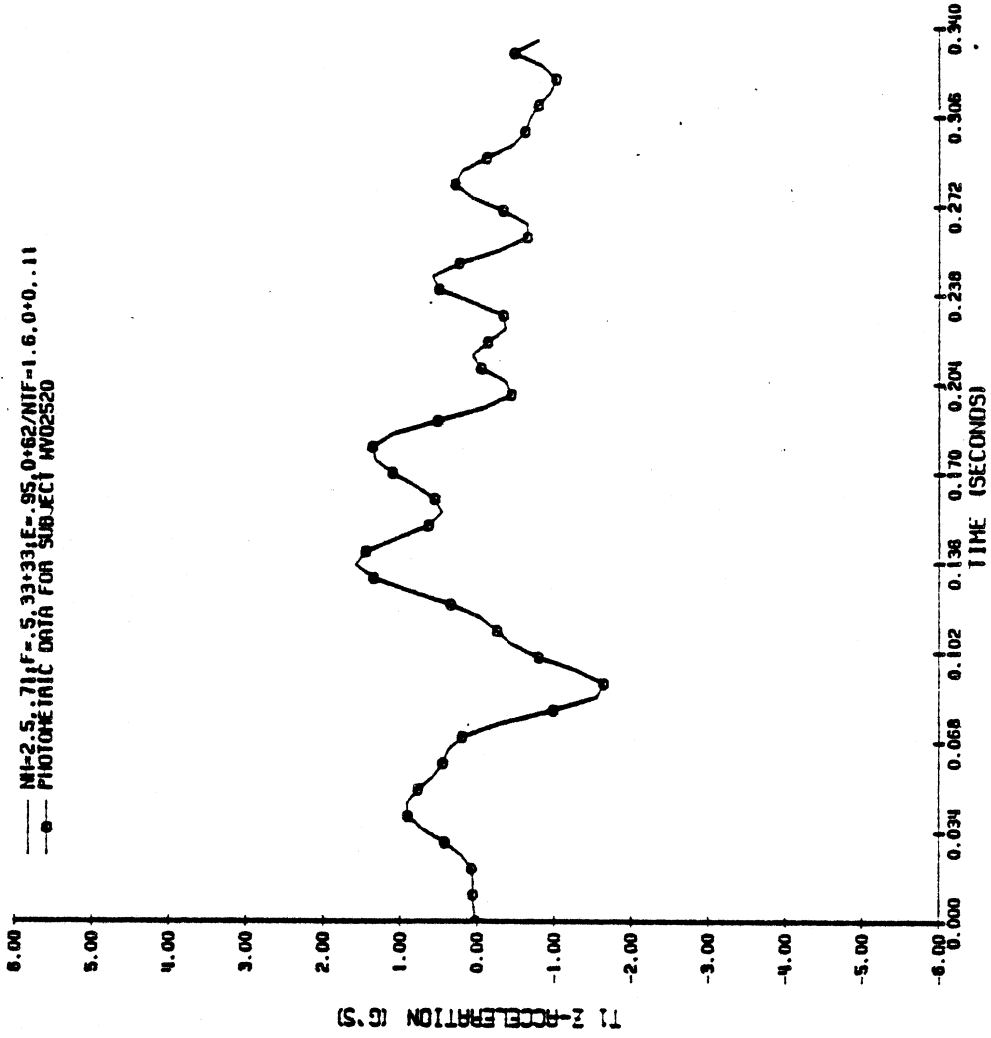


FIGURE 23. T1 Z-ACCELERATION DOT453.

3-HEAD ANGULAR POSITION  
WAYNE STATE DOT.453. -GX AT 5 G'S  
TI MOTION FORCED

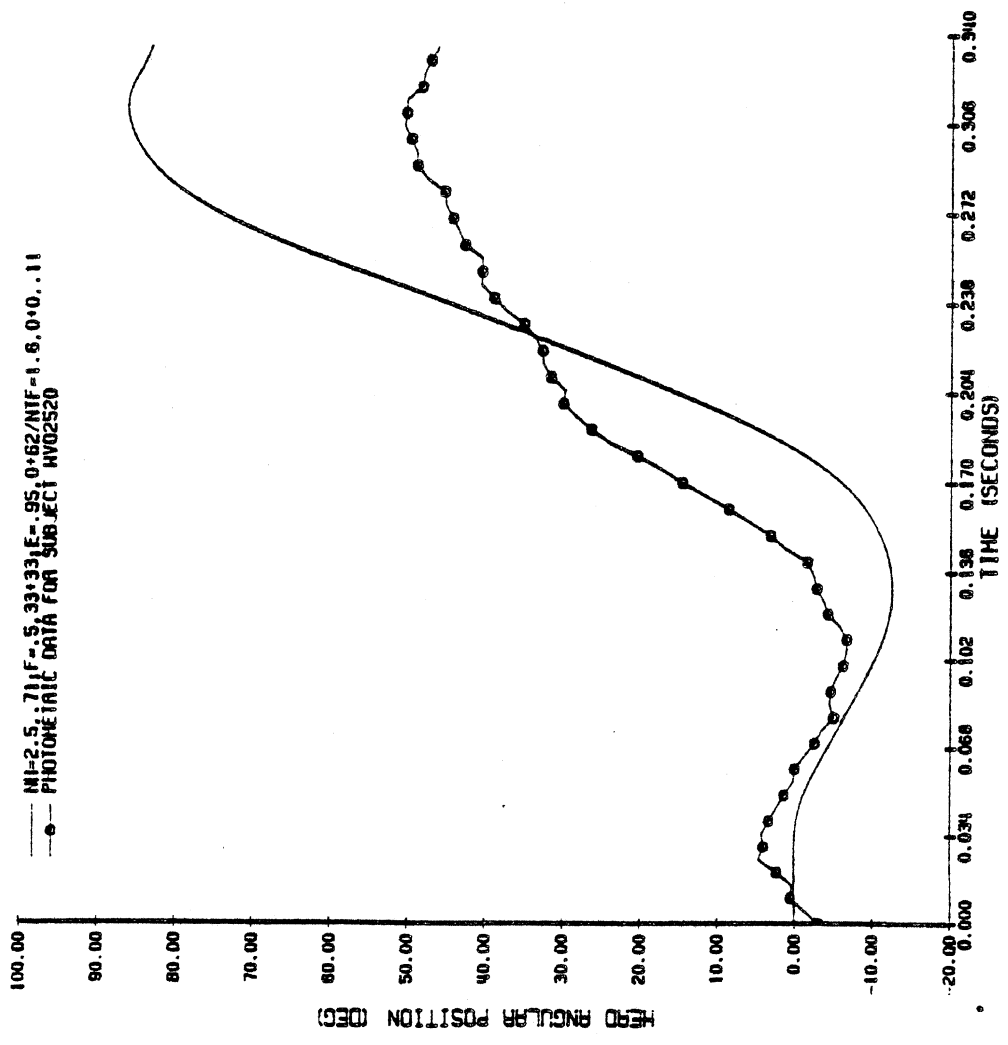


FIGURE 24. HEAD ANGULAR POSITION FOR NBDL ADJUSTED PARAMETERS DOT453.

4-HEAD ANGULAR VELOCITY  
WAYNE STATE DOT.453. -GX AT 5 G'S  
TI MOTION FORCED

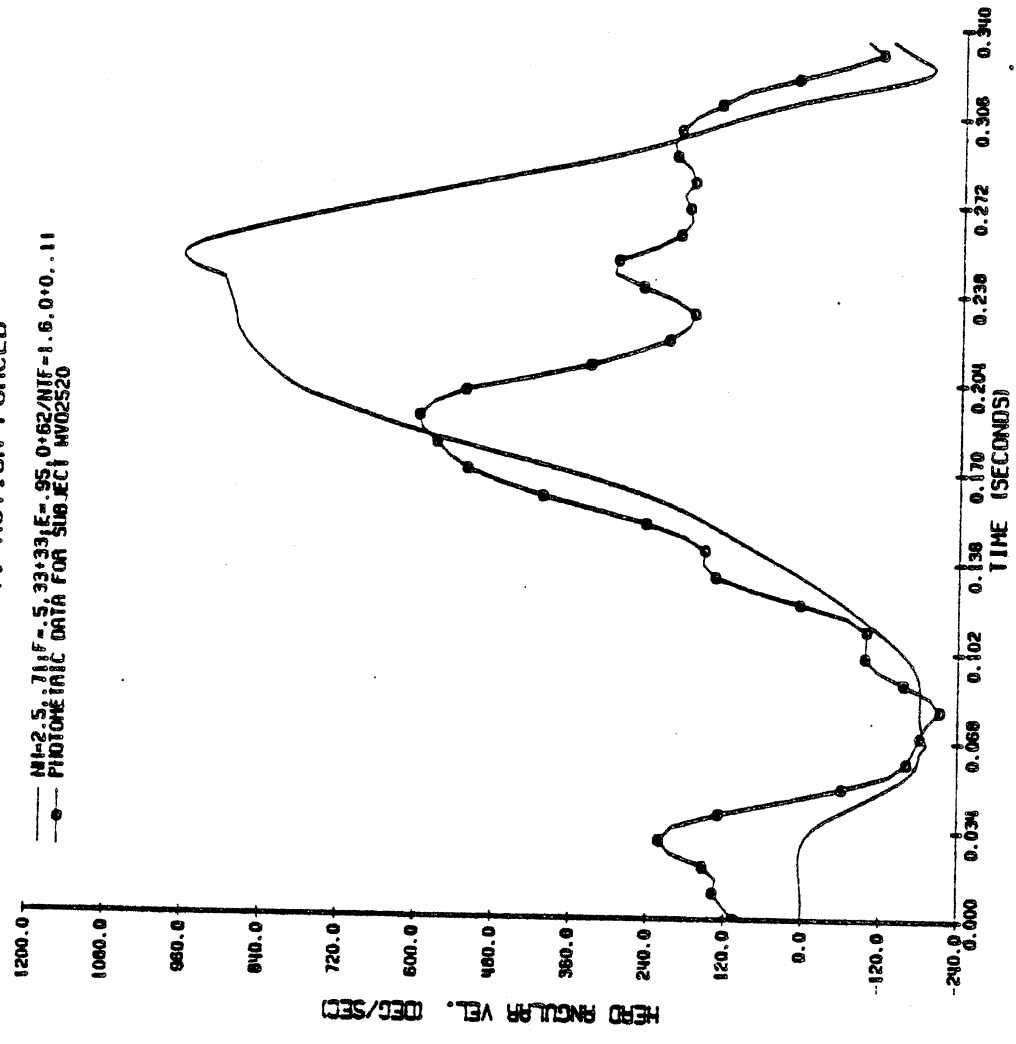


FIGURE 25. HEAD ANGULAR VELOCITY FOR NBDL ADJUSTED PARAMETERS DOT453.

5--HEAD ANGULAR ACCELERATION  
WAYNE STATE DOT.453, -GX AT 5 G'S  
T1 MOTION FORCED

NI=2.5, 711F=.5, 33\*33, E=.95, 0\*62/NIF=1.6, 0\*0..11  
PHOTOMETRIC DATA FOR SUBJECT W02520

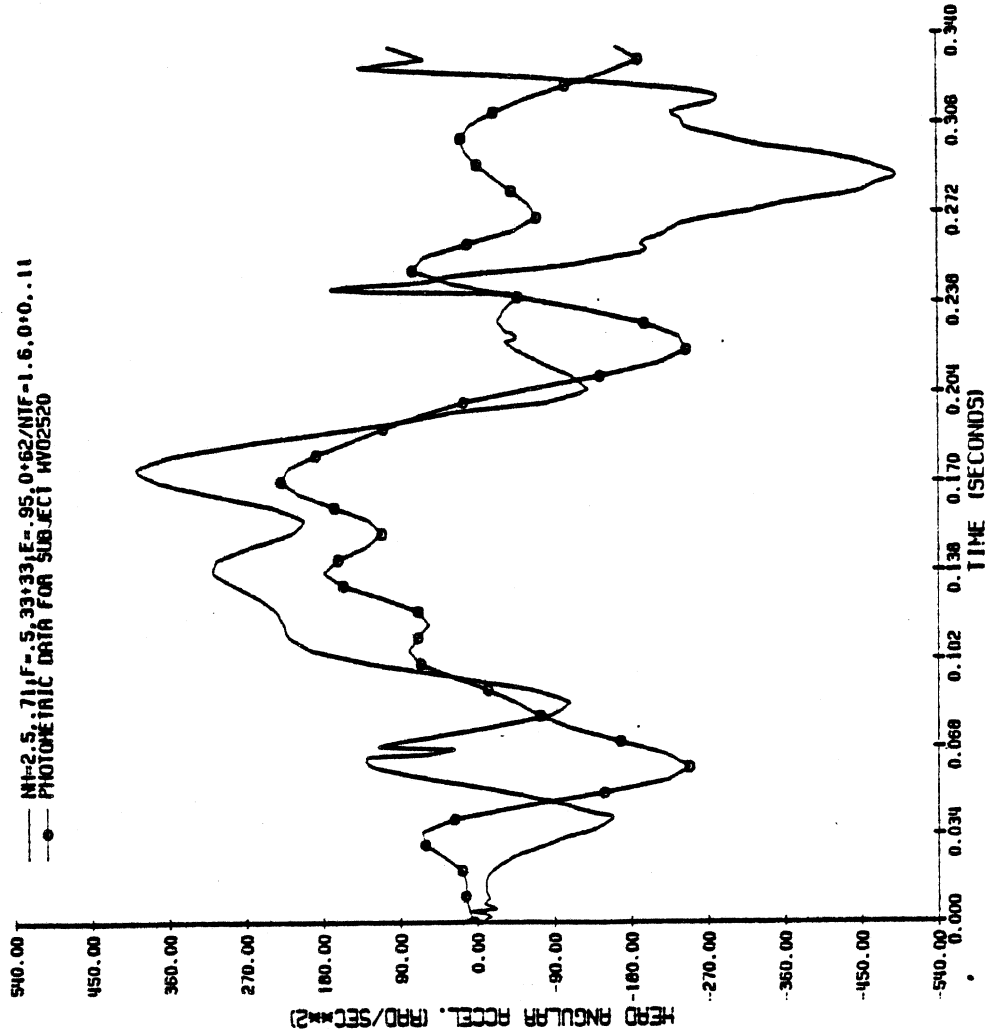


FIGURE 26. HEAD ANGULAR ACCELERATION FOR NBDL ADJUSTED PARAMETERS DOT453.

6--RESULT. LINEAR ACCEL. OF HEAD ANATOMICAL ORIGIN  
WAYNE STATE DOT.453, -GX AT 5 G'S  
T1 MOTION FORCED

NI=2.5, 711F=.5, 33\*33, E=.95, 0\*62/NIF=1.6, 0\*0..11  
PHOTOMETRIC DATA FOR SUBJECT W02520

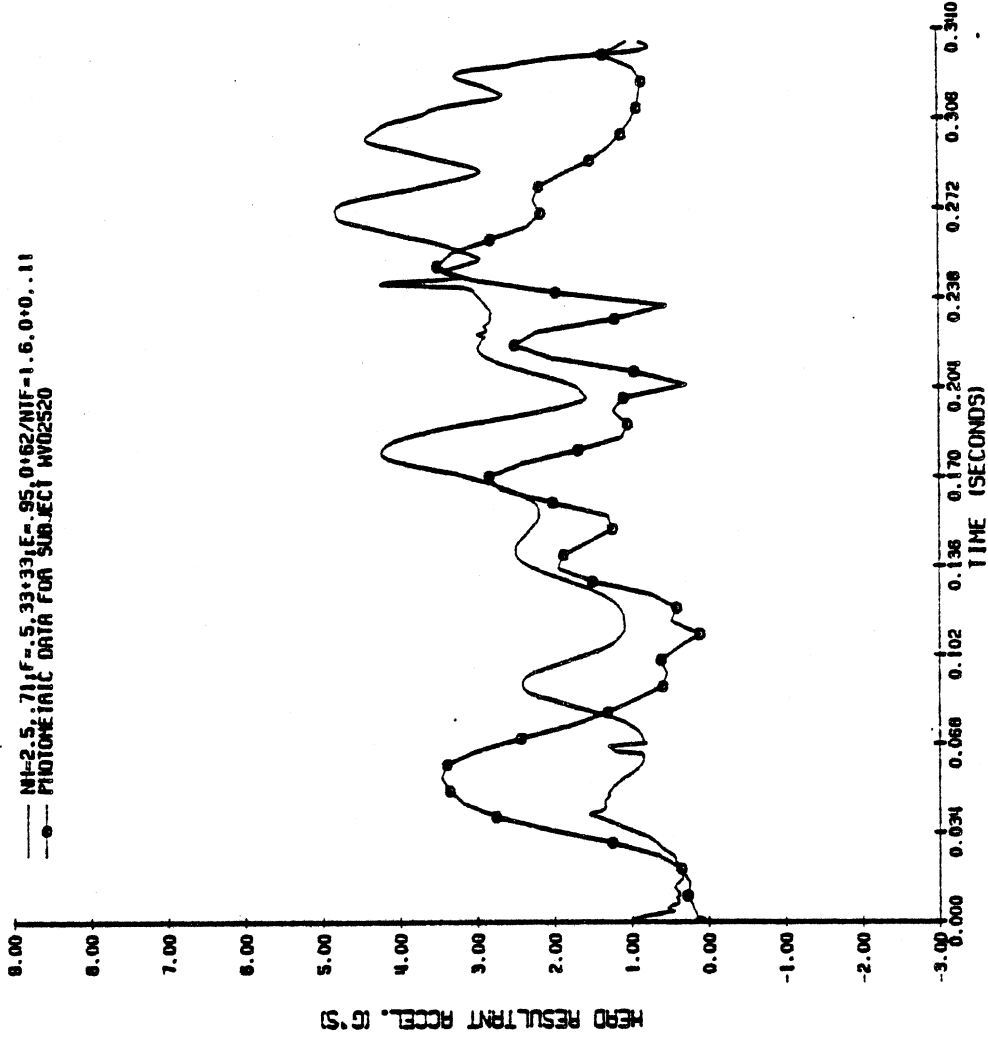


FIGURE 27. RESULTANT LINEAR ACCELERATION OF HEAD FOR NBDL ADJUSTED PARAMETERS DOT453.

19-UPPER NECK MOMENT VS. ANGLE  
 WAYNE STATE DOT.453, -GX AT 5 G'S  
 T1 MOTION FORCED

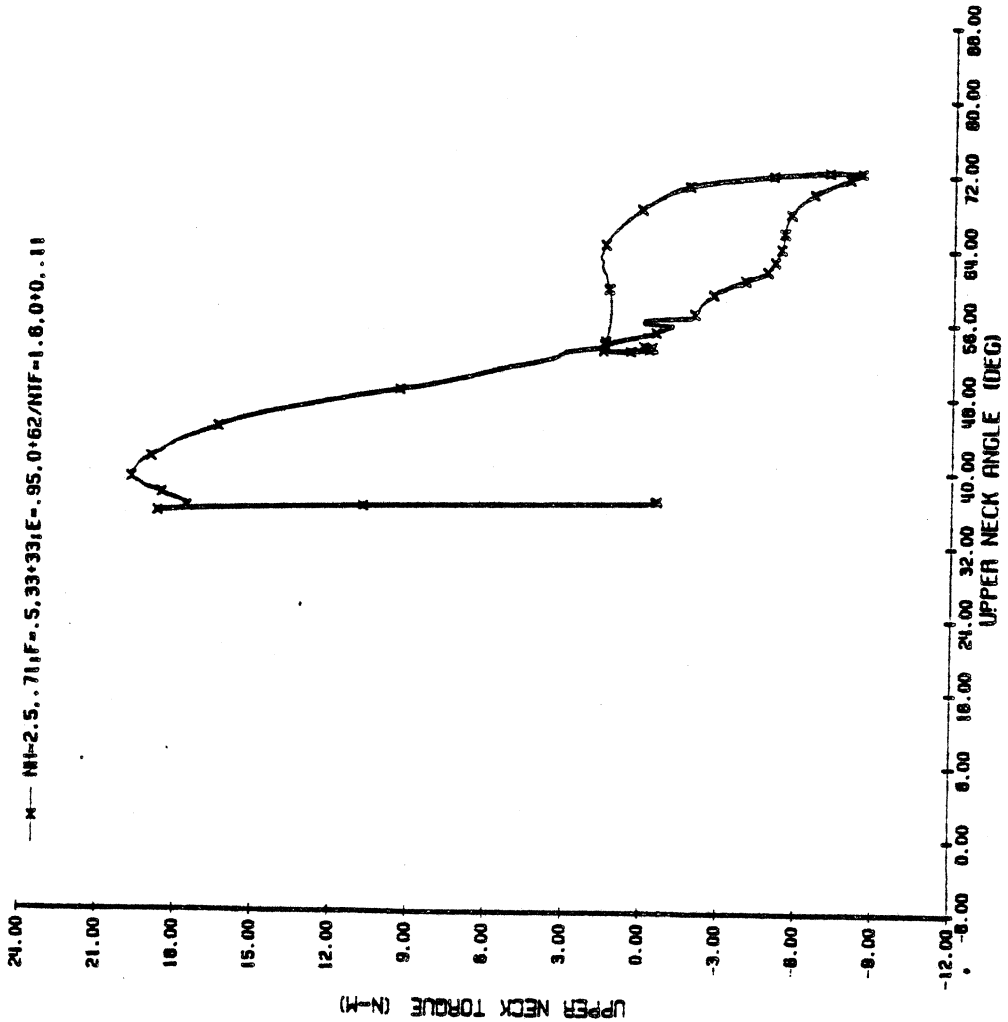


FIGURE 28. UPPER NECK MOMENT VS. NECK ANGLE FOR NBDL. ADJUSTED PARAMETERS DOT453.

20-LOWER NECK MOMENT VS. ANGLE  
 WAYNE STATE DOT.453, -GX AT 5 G'S  
 T1 MOTION FORCED

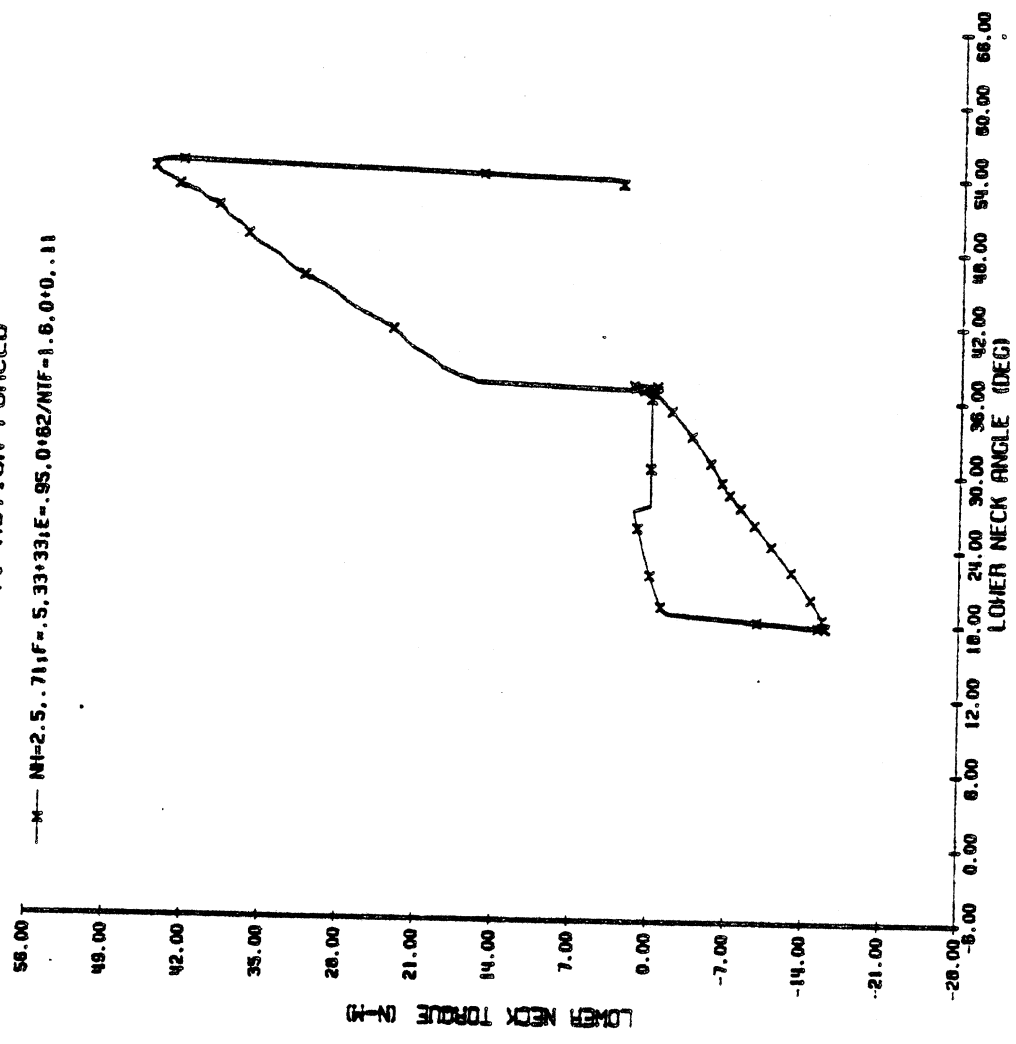


FIGURE 29. LOWER NECK MOMENT VS. NECK ANGLE FOR NBDL. ADJUSTED PARAMETERS DOT453.

21-HEAD ANGLE VS. NECK ANGLE  
 WAYNE STATE DOT.453, -GX AT 5 G'S  
 T1 MOTION FORCED

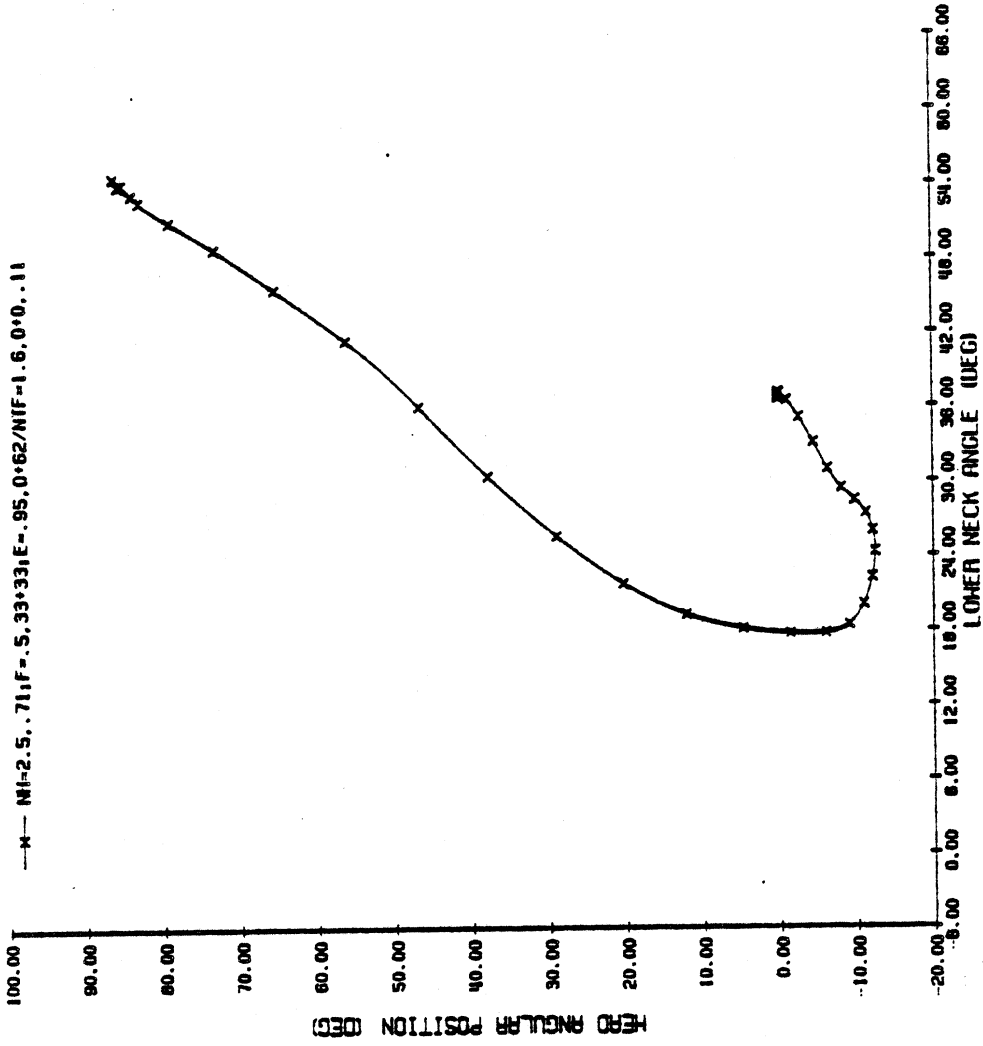


FIGURE 30. HEAD ANGLE VS. NECK ANGLE FOR NBDL ADJUSTED  
 PARAMETERS DOT453.

1-11 X-ACCELERATION  
 WAYNE STATE DOT.454, -GX AT 5 G'S  
 T1 MOTION FORCED

MI-2.5, 71; F=.5, 33; 33; E=.95, 0.62/NIF-1.6, 0\*0. .11  
 PHOTOEITIC DATA FOR SUBJECT W02520

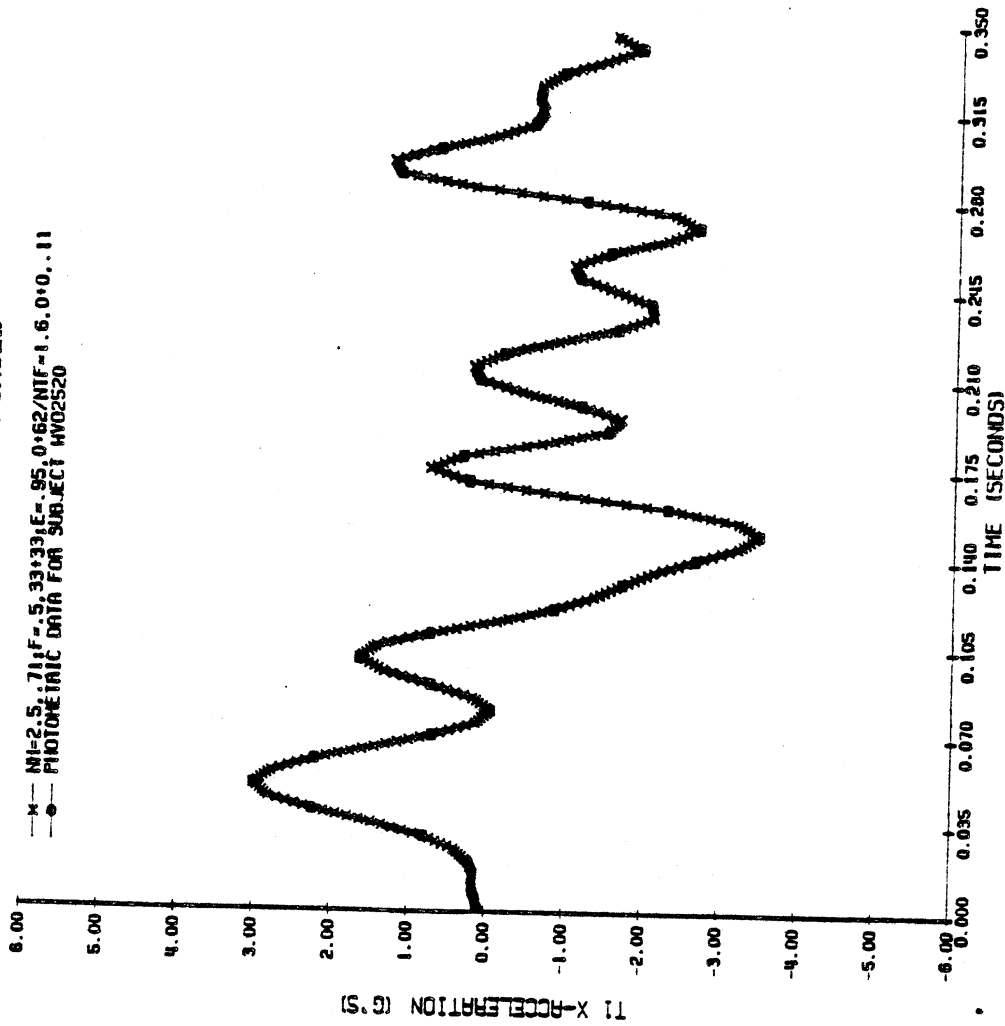


FIGURE 31. T1 X-ACCELERATION DOT454.

2-11 Z-ACCELERATION  
 WAYNE STATE DOT.454, -GX AT 5 G'S  
 T1 MOTION FORCED

MI-2.5, 71; F=.5, 33; 33; E=.95, 0.62/NIF-1.6, 0\*0. .11  
 PHOTOEITIC DATA FOR SUBJECT W02520

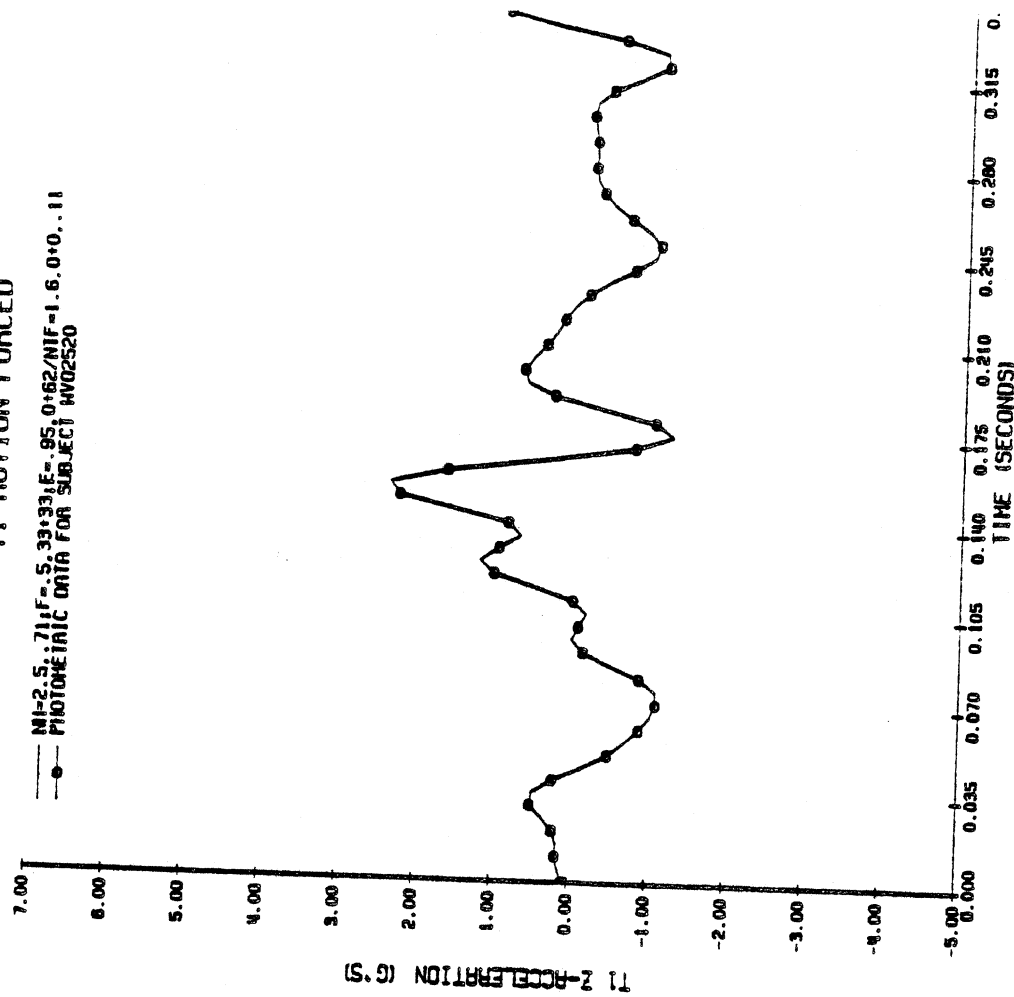


FIGURE 32. T1 Z-ACCELERATION DOT454.



3-HEAD ANGULAR POSITION  
 WAYNE STATE DOT 454, -GX AT 5 G'S  
 11 MOTION FORCED

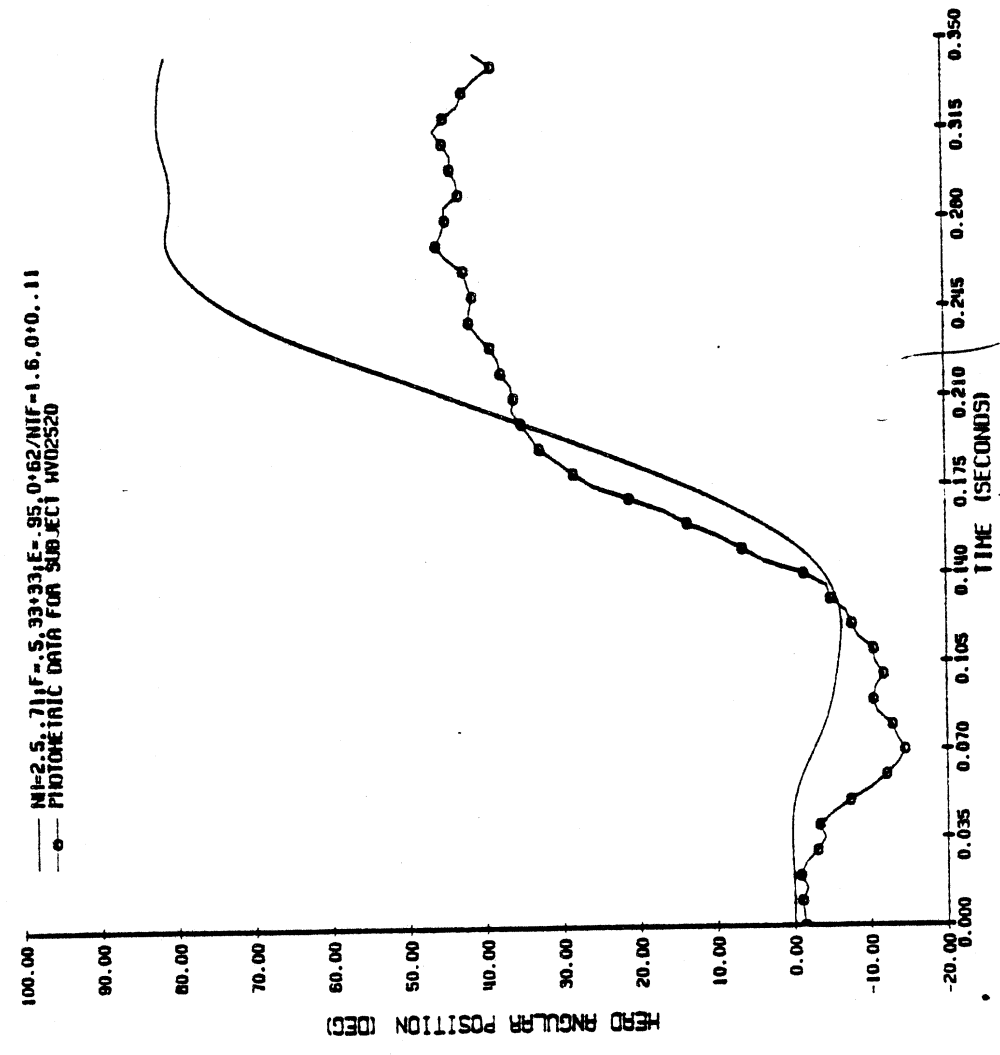


FIGURE 33. HEAD ANGULAR POSITION FOR NBDL ADJUSTED PARAMETERS DOT454.

4-HEAD ANGULAR VELOCITY  
 WAYNE STATE DOT 454, -GX AT 5 G'S  
 11 MOTION FORCED

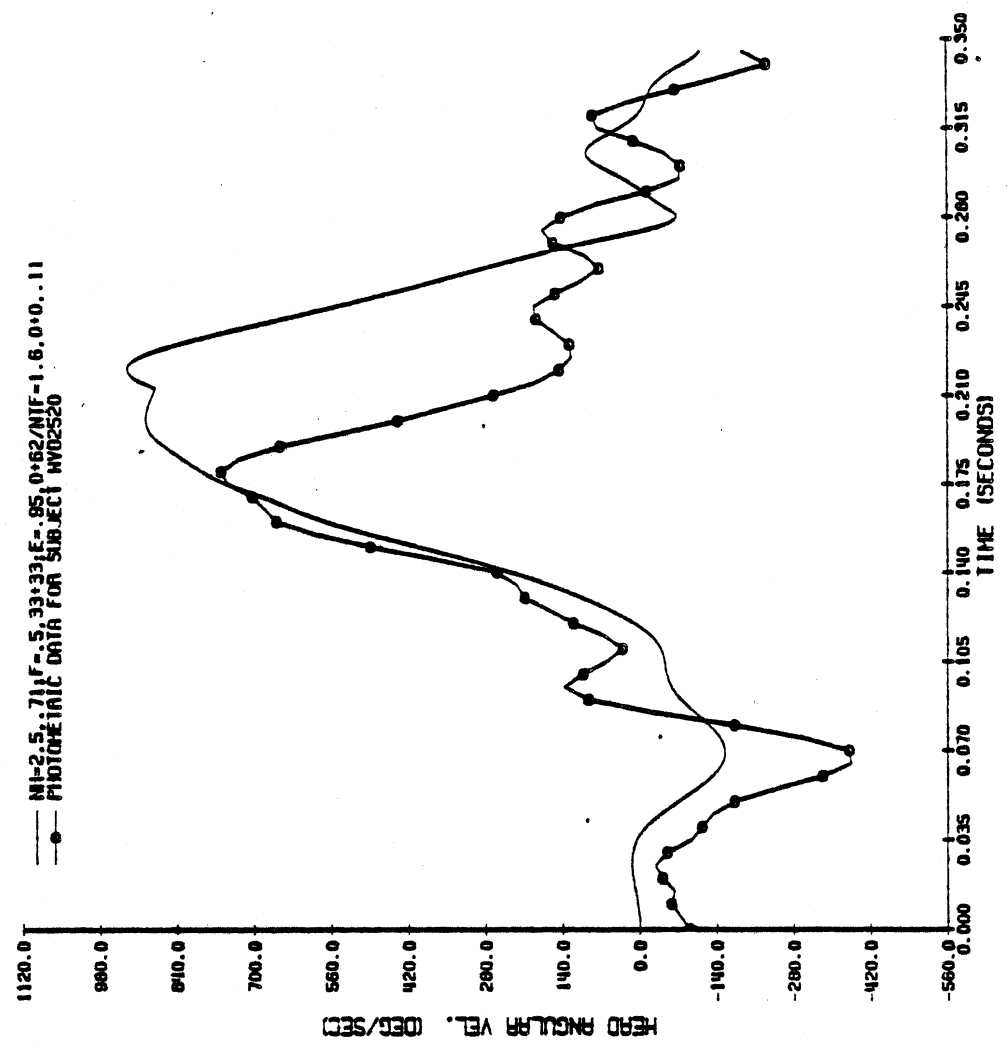


FIGURE 34. HEAD ANGULAR VELOCITY FOR NBDL ADJUSTED PARAMETERS DOT454.

5-HEAD ANGULAR ACCELERATION  
 WAYNE STATE DOT 454  
 -GX AT 5 G'S  
 11 MOTION FORCED

NI-2.5.71F-5.33+33E-.95.0+62/NIF-1.6.0+0..11  
 PHOTOGRAPHIC DATA FOR SUBJECT MVD2520

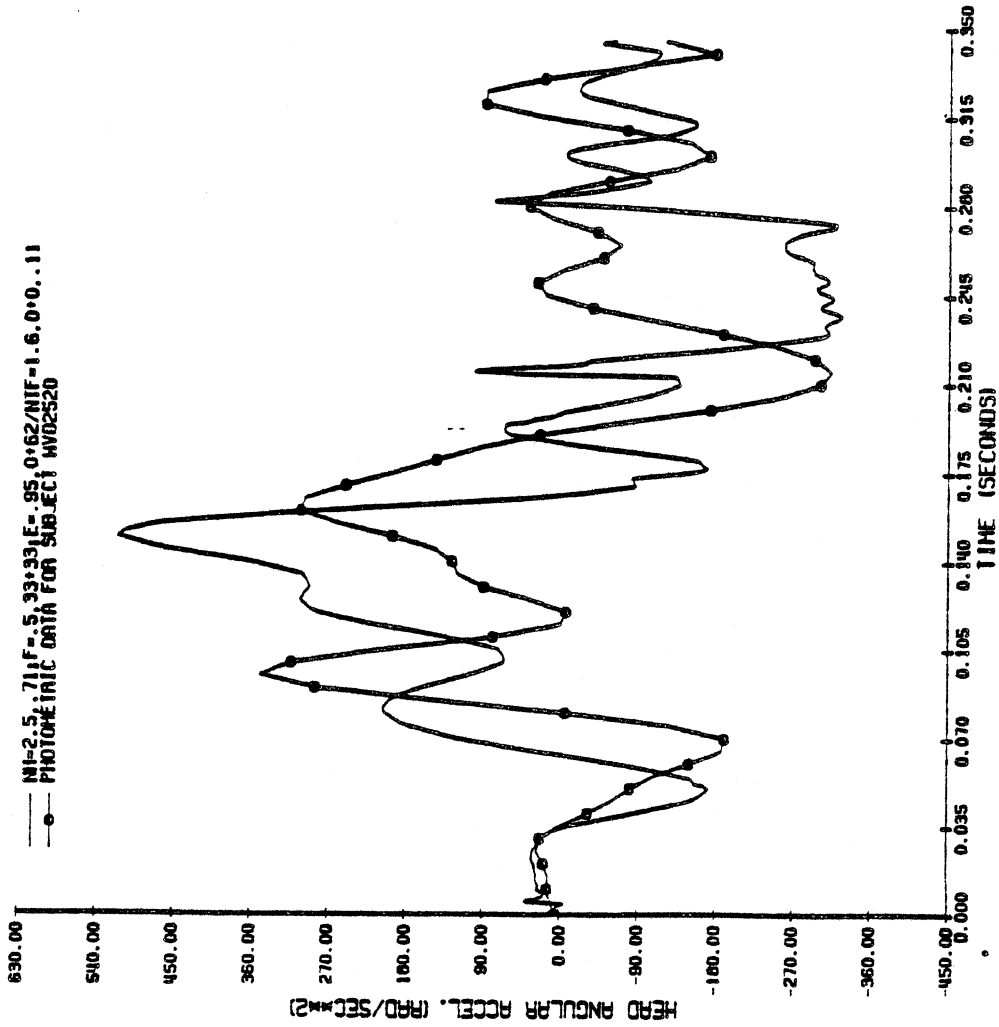


FIGURE 35. HEAD ANGULAR ACCELERATION FOR NBDL ADJUSTED PARAMETERS DOT454.

6-RESULT. LINEAR ACCEL. OF HEAD ANATOMICAL ORIGIN  
 WAYNE STATE DOT 454  
 -GX AT 5 G'S  
 11 MOTION FORCED

NI-2.5.71F-5.33+33E-.95.0+62/NIF-1.6.0+0..11  
 PHOTOGRAPHIC DATA FOR SUBJECT MVD2520

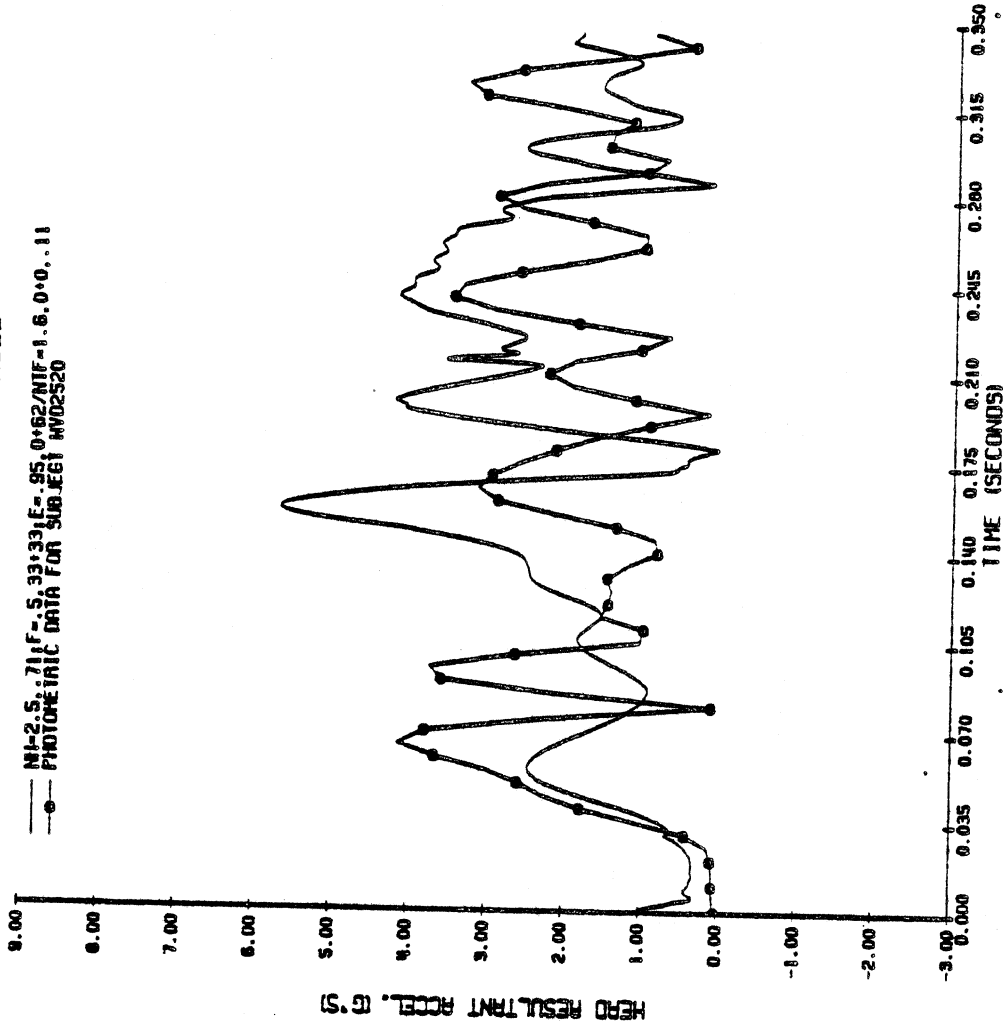


FIGURE 36. RESULTANT LINEAR ACCELERATION OF HEAD FOR NBDL ADJUSTED PARAMETERS DOT454.

19-UPPER NECK MOMENT VS. ANGLE  
 WAYNE STATE DOT.454, -GX AT 5 G'S  
 T1 MOTION FORCED

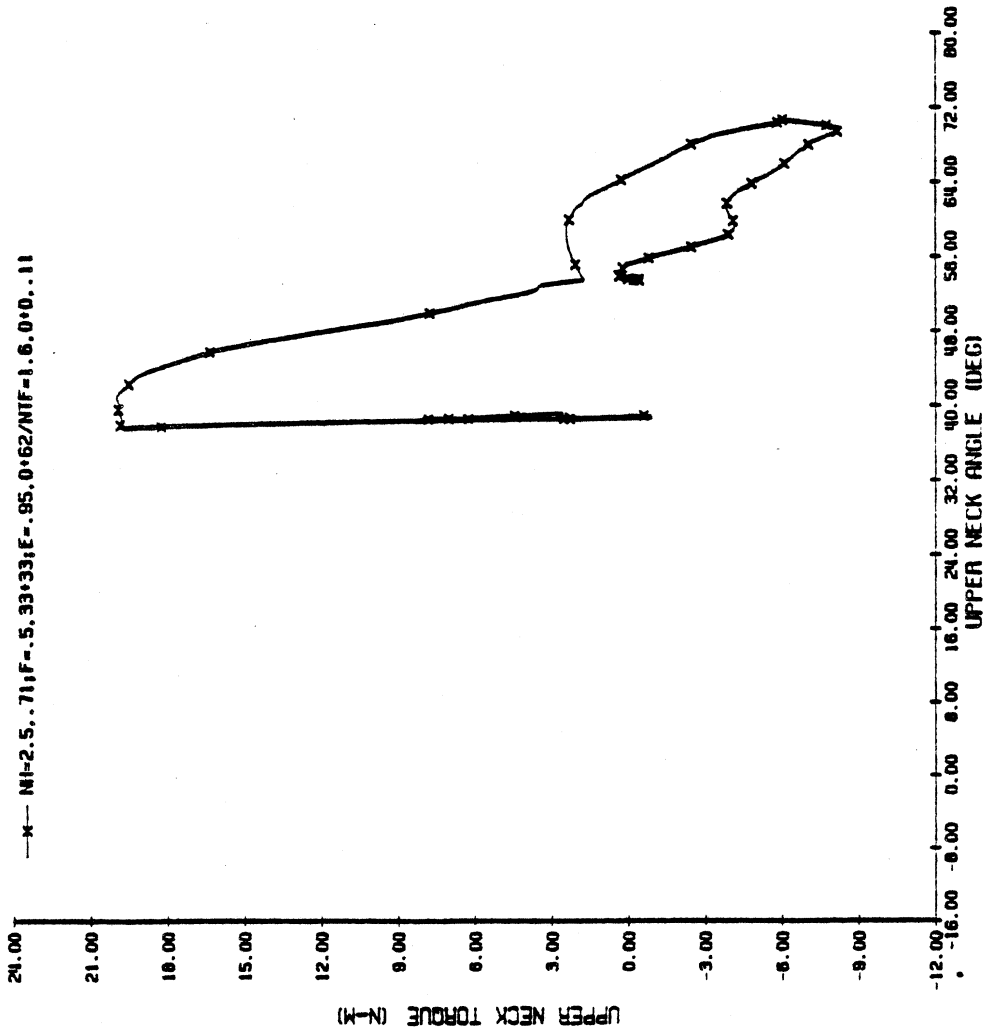


FIGURE 37. UPPER NECK MOMENT VS. NECK ANGLE FOR NBDL ADJUSTED PARAMETERS DOT454.

20-LOWER NECK MOMENT VS. ANGLE  
 WAYNE STATE DOT.454, -GX AT 5 G'S  
 T1 MOTION FORCED

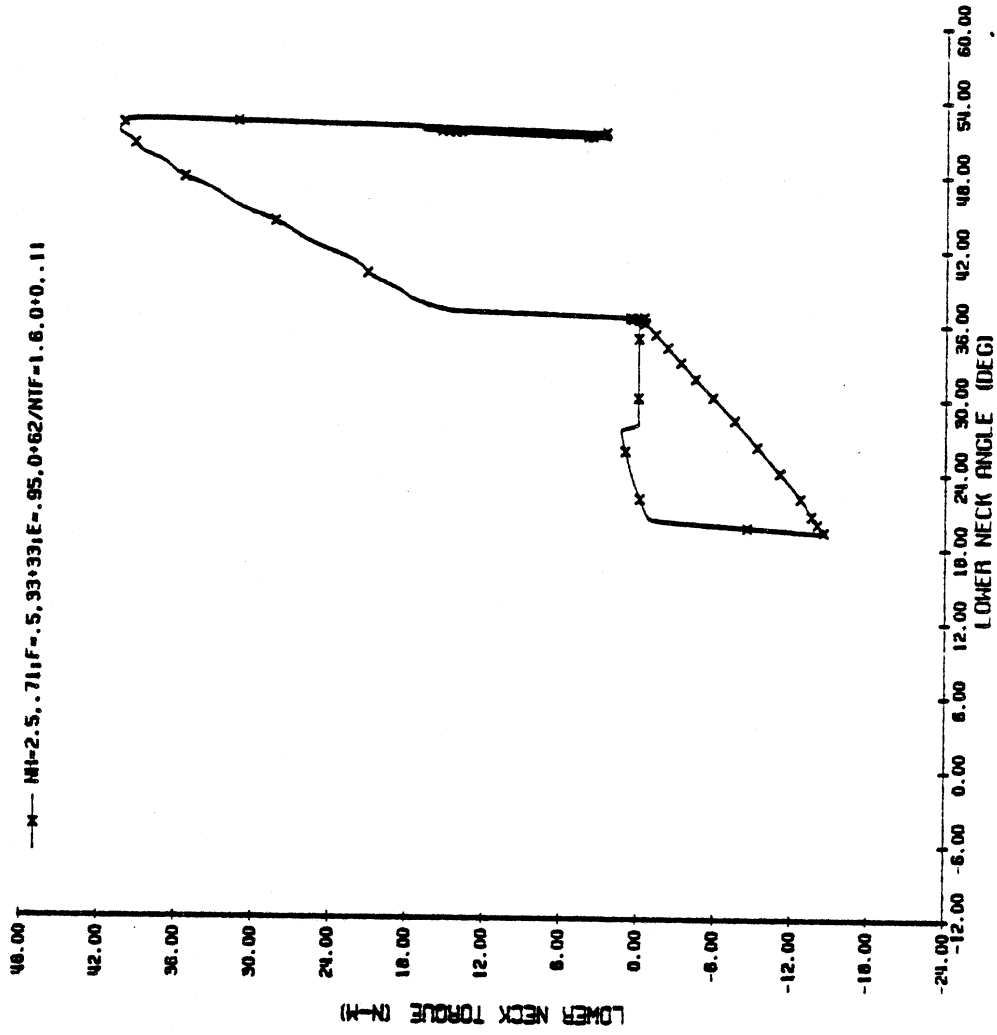


FIGURE 38. LOWER NECK MOMENT VS. NECK ANGLE FOR NBDL ADJUSTED PARAMETERS DOT454.

21-HEAD ANGLE VS. NECK ANGLE  
 WAYNE STATE DOT 454 -GX AT 5 G'S  
 T1 MOTION FORCED

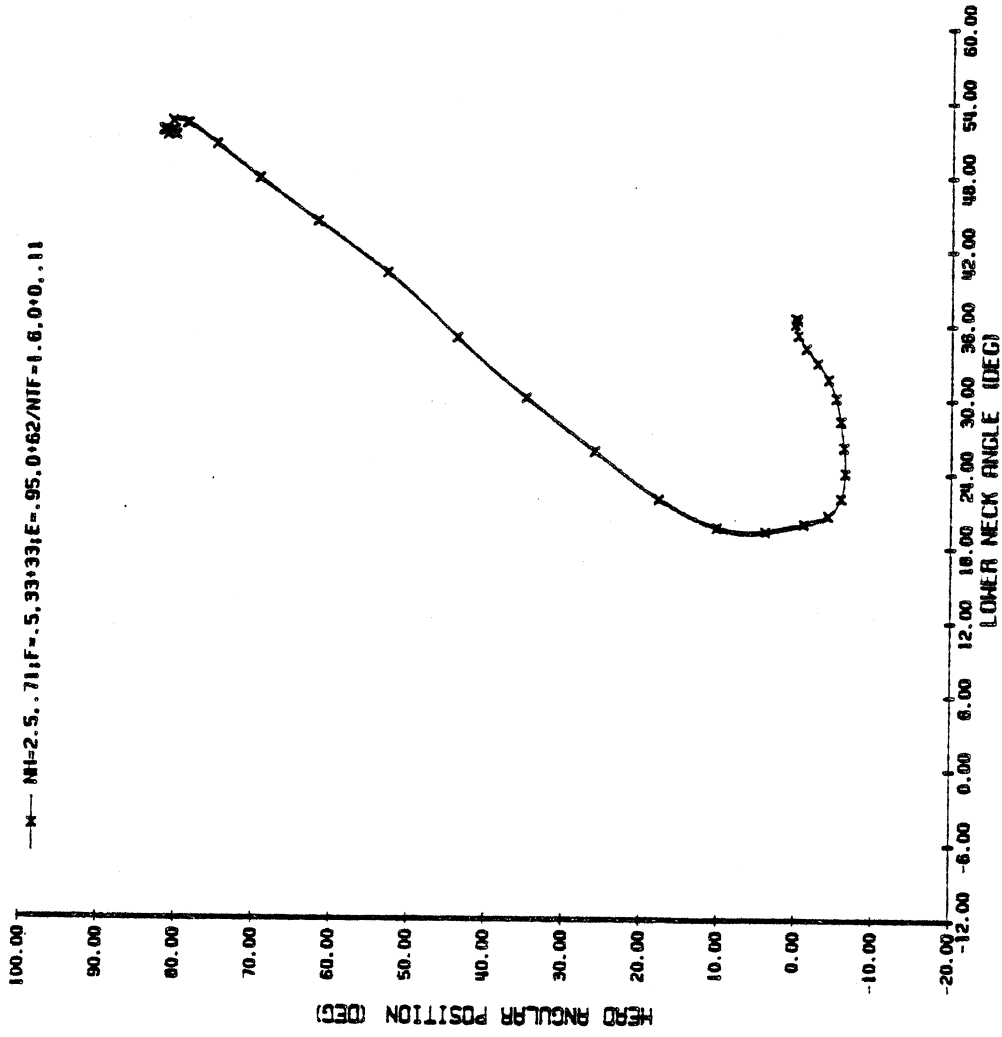


FIGURE 39. HEAD ANGLE VS. NECK ANGLE FOR NBDL ADJUSTED PARAMETERS DOT454.

1-T1 X-ACCELERATION  
 WAYNE STATE DOT.455, -GX AT 5 G'S  
 T1 MOTION FORCED

M=2.5, 711F=5.33+331E=.95, 0+62/NIF=1.6, 0+0.11  
 PHOTOGRAPHIC DATA FOR SUBJECT HW02520

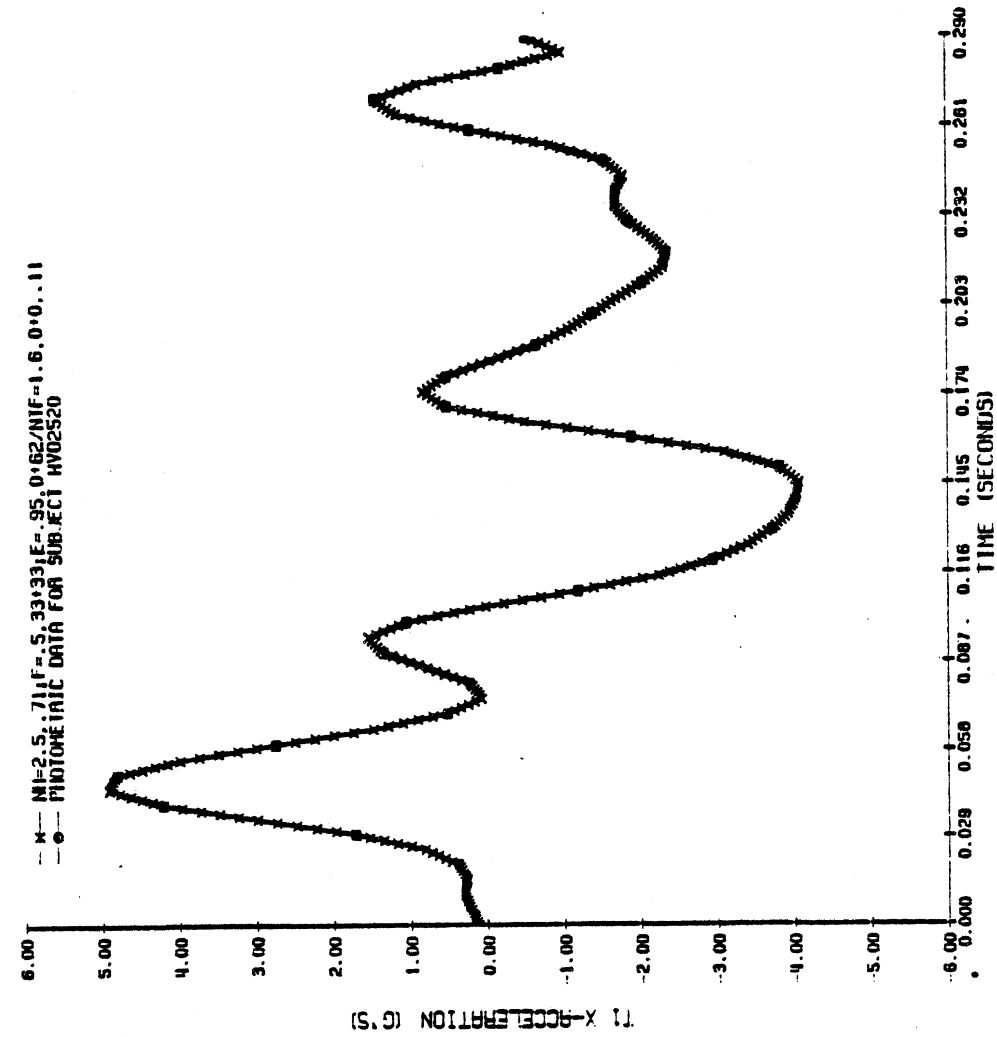


FIGURE 40. T1 X-ACCELERATION DOT455.

2-T1 Z-ACCELERATION  
 WAYNE STATE DOT.455, -GX AT 5 G'S  
 T1 MOTION FORCED

M=2.5, 711F=5.33+331E=.95, 0+62/NIF=1.6, 0+0.11  
 PHOTOGRAPHIC DATA FOR SUBJECT HW02520

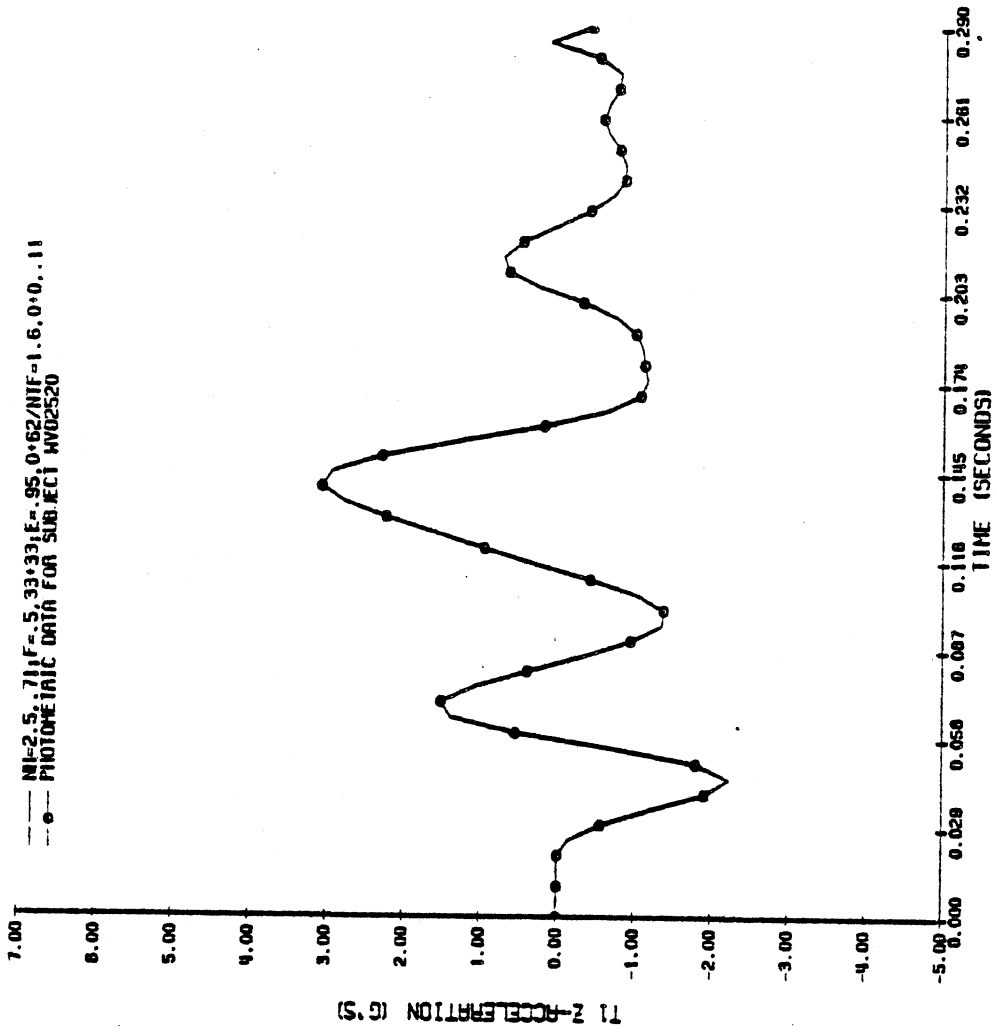


FIGURE 41. T1 Z-ACCELERATION DOT455.

3-HEAD ANGULAR POSITION  
WAYNE STATE DOT.455, -GX AT 5 G'S  
T1 MOTION FORCED

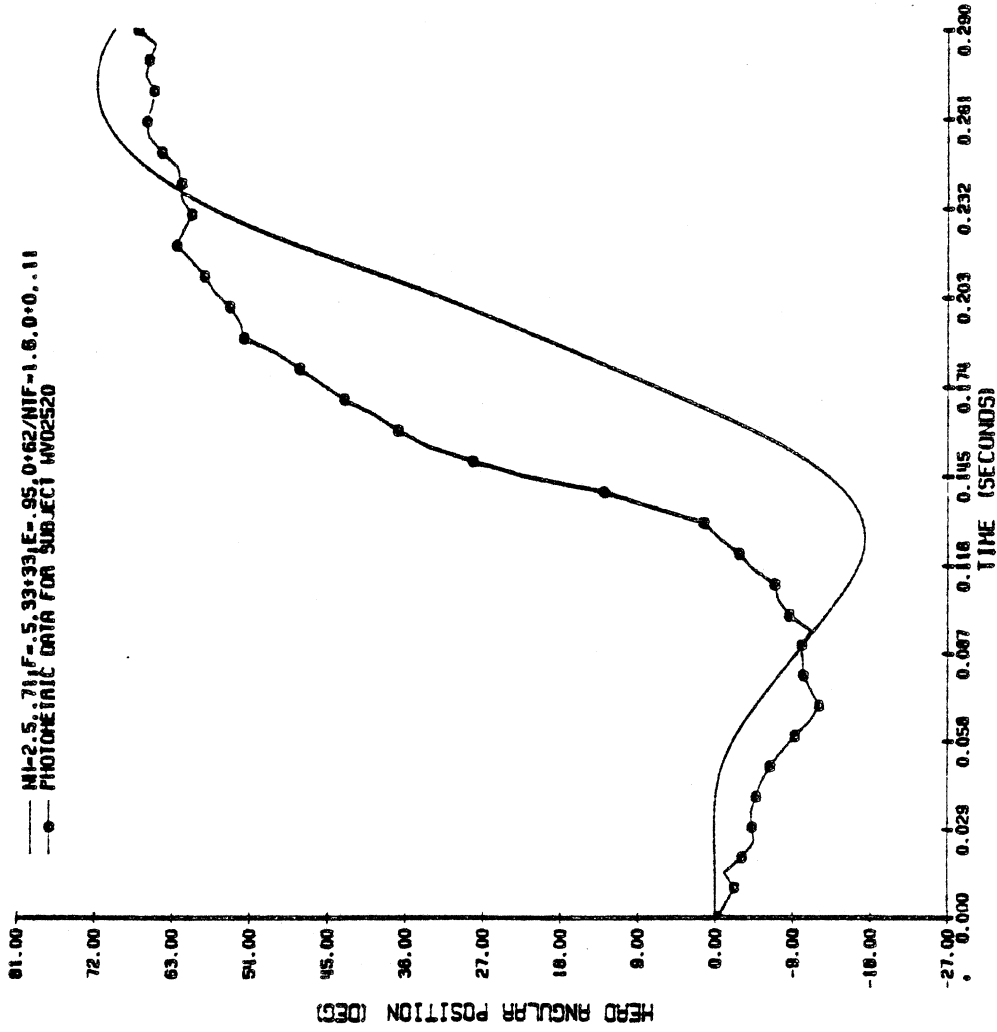


FIGURE 42. HEAD ANGULAR POSITION FOR NBDL ADJUSTED PARAMETERS DOT455.

4-HEAD ANGULAR VELOCITY  
WAYNE STATE DOT.455, -GX AT 5 G'S  
T1 MOTION FORCED

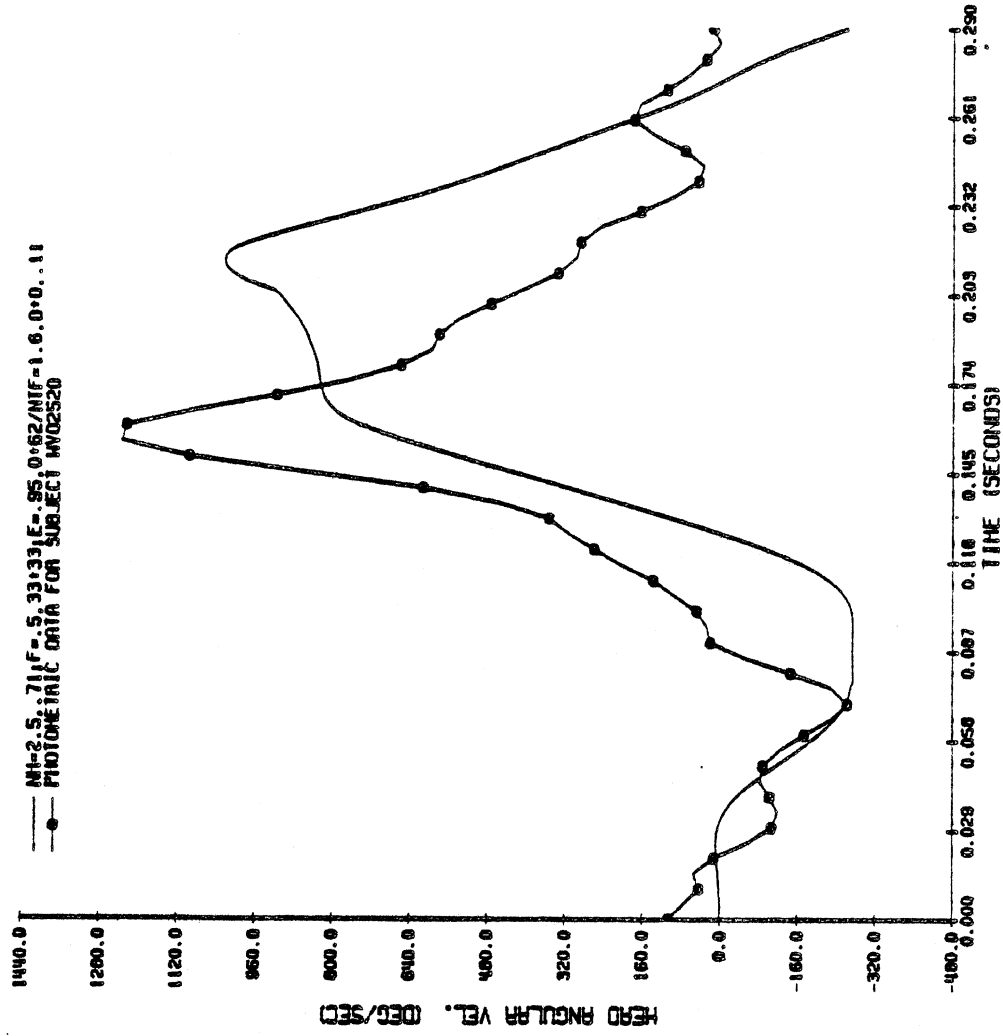


FIGURE 43. HEAD ANGULAR VELOCITY FOR NBDL ADJUSTED PARAMETERS DOT455.

5-HEAD ANGULAR ACCELERATION  
WAYNE STATE DOT.455, -GX AT 5 G'S  
T1 MOTION FORCED

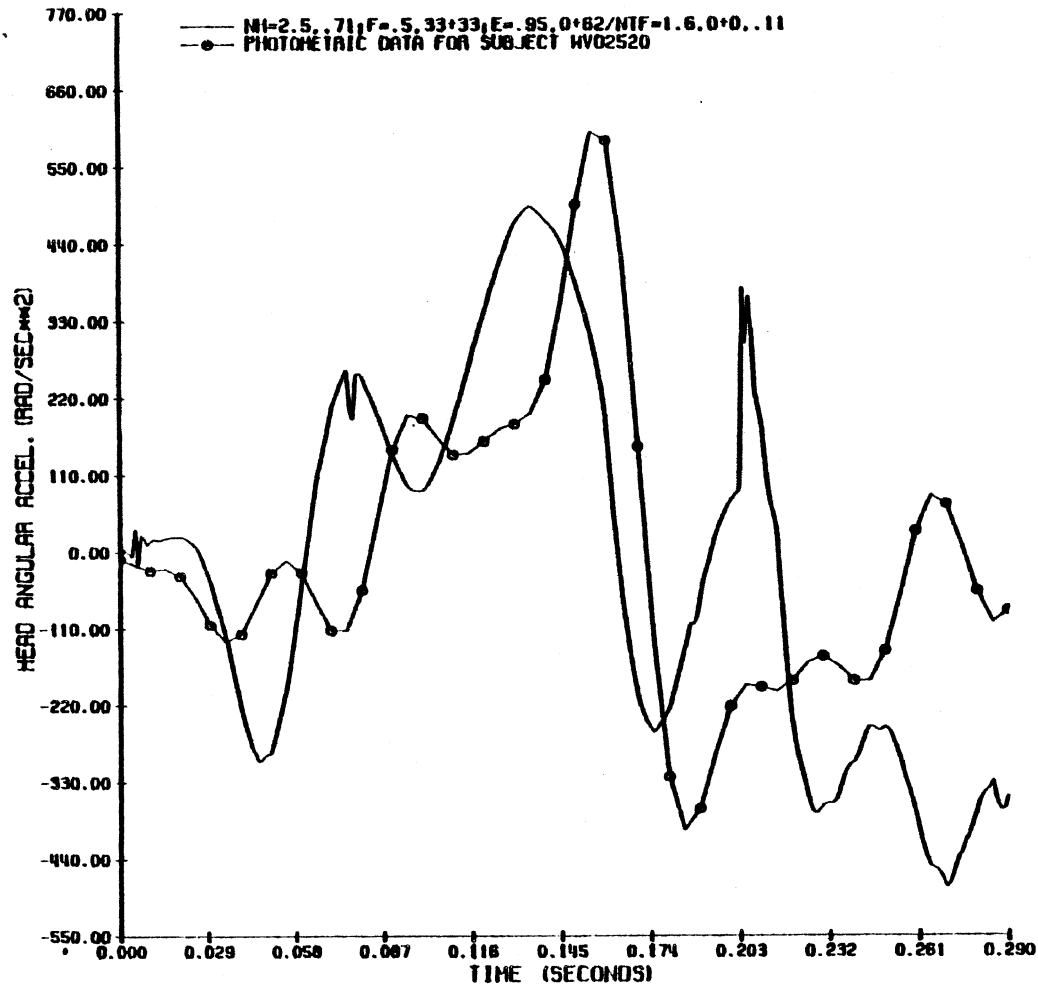


FIGURE 44. HEAD ANGULAR ACCELERATION FOR NBDL ADJUSTED PARAMETERS DOT455.

6-RESUL. LINEAR ACCEL. OF HEAD ANATOMICAL ORIGIN  
WAYNE STATE DOT.455, -GX AT 5 G'S  
T1 MOTION FORCED

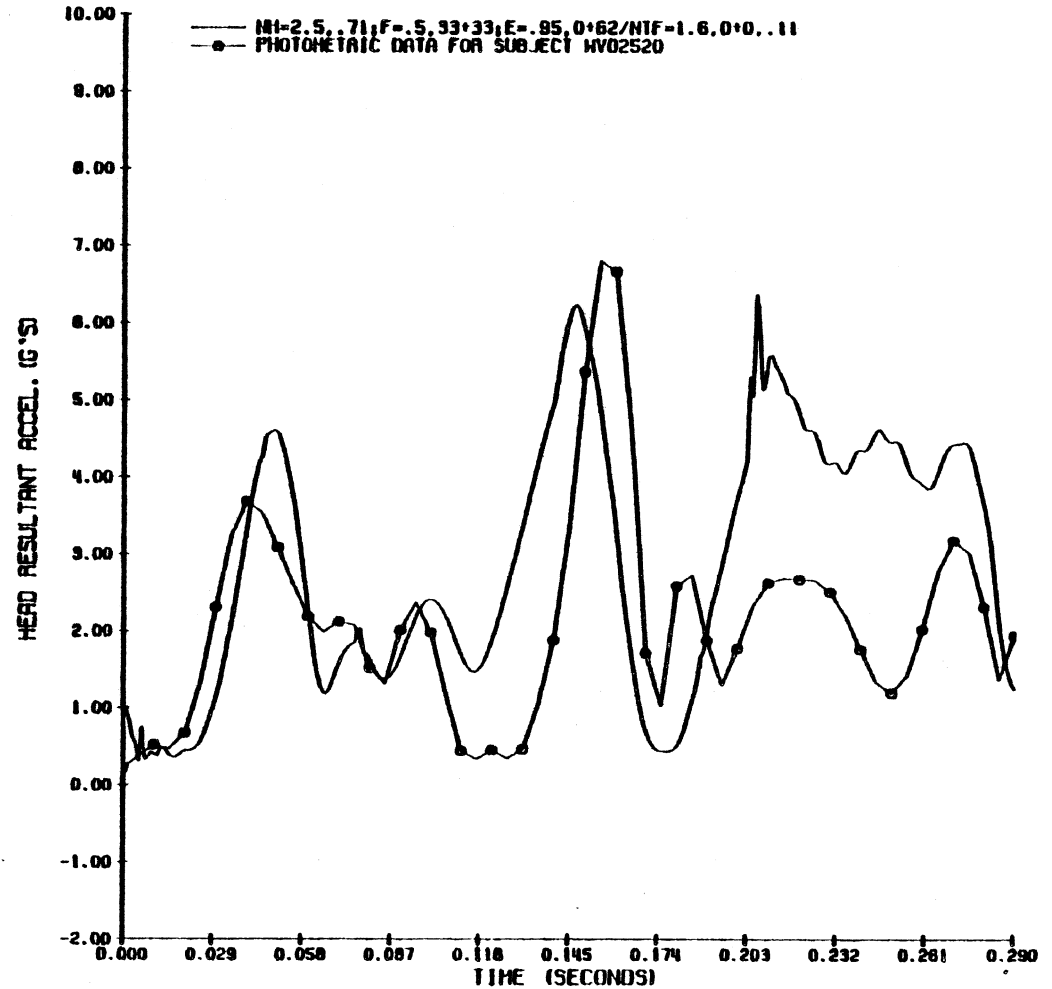


FIGURE 45. RESULTANT LINEAR ACCELERATION OF HEAD FOR NBDL ADJUSTED PARAMETERS DOT455.

19-UPPER NECK MOMENT VS. ANGLE  
 WAYNE STATE DOT.455, -GX AT 5 G'S  
 T1 MOTION FORCED

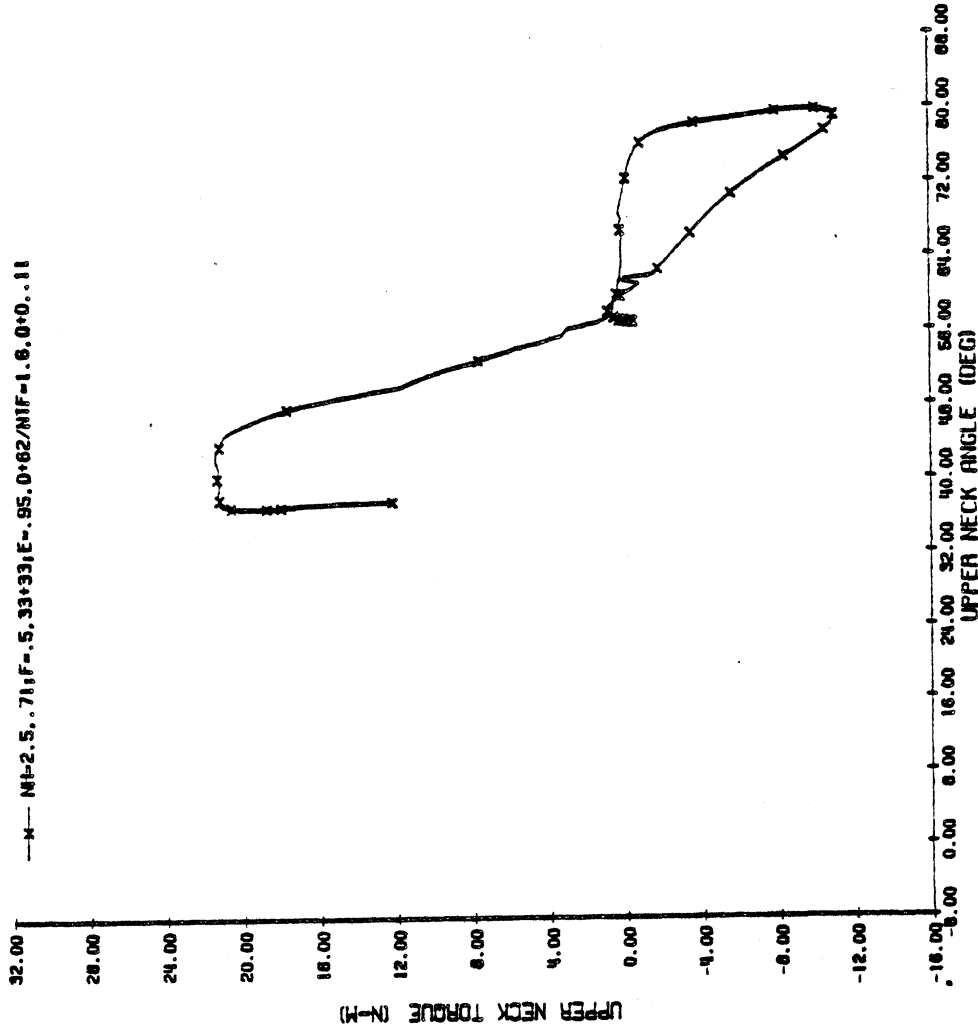


FIGURE 46. UPPER NECK MOMENT VS. NECK ANGLE FOR NBDL ADJUSTED PARAMETERS DOT455.

20-LOWER NECK MOMENT VS. ANGLE  
 WAYNE STATE DOT.455, -GX AT 5 G'S  
 T1 MOTION FORCED

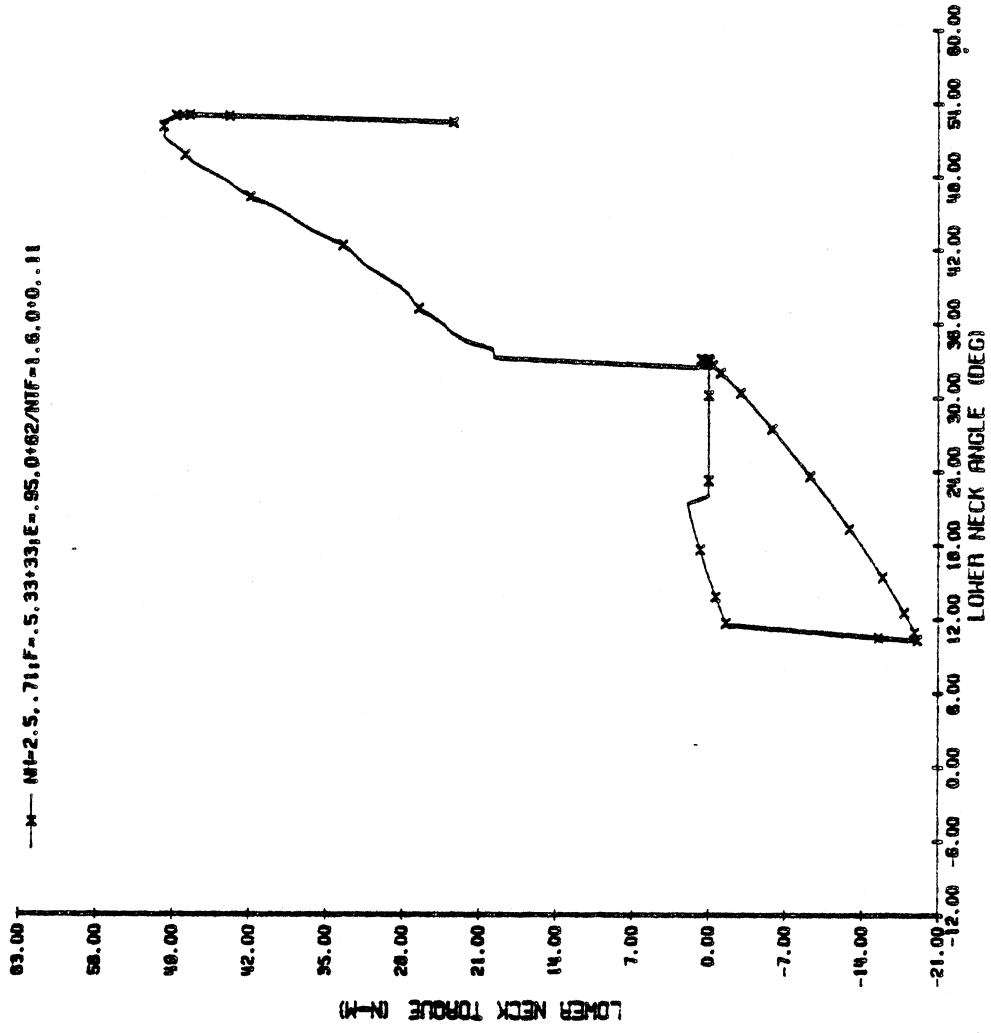


FIGURE 47. LOWER NECK MOMENT VS. NECK ANGLE FOR NBDL ADJUSTED PARAMETERS DOT455.





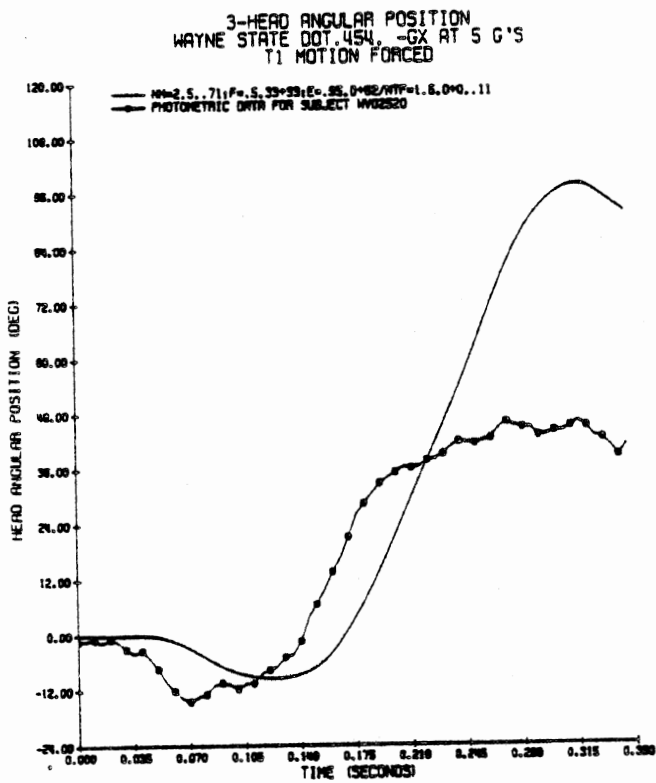


FIGURE 49. HEAD ANGULAR POSITION WITH NBDL FLEXION STIFFNESS DOT454.

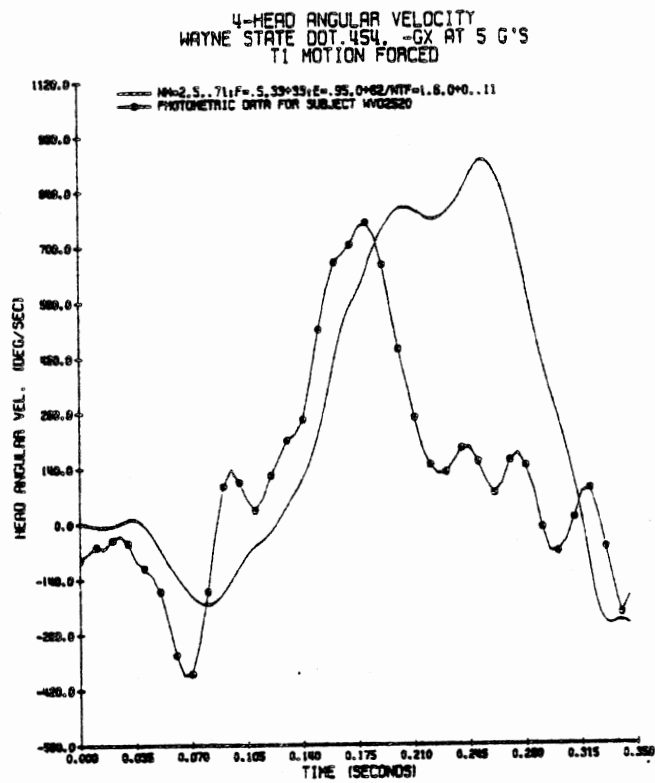


FIGURE 50. HEAD ANGULAR VELOCITY WITH NBDL FLEXION STIFFNESS DOT454.

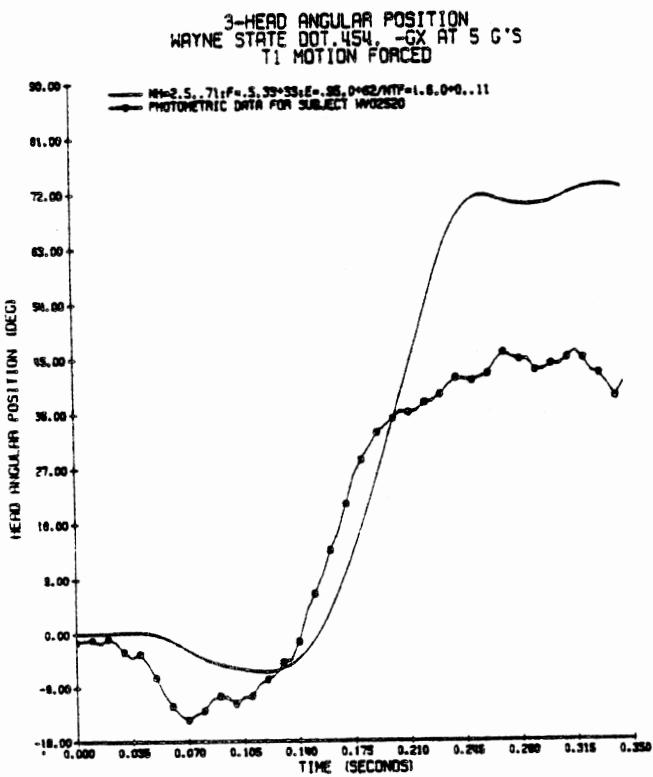


FIGURE 51. HEAD ANGULAR POSITION WITH INCREASED FLEXION STIFFNESS DOT454.

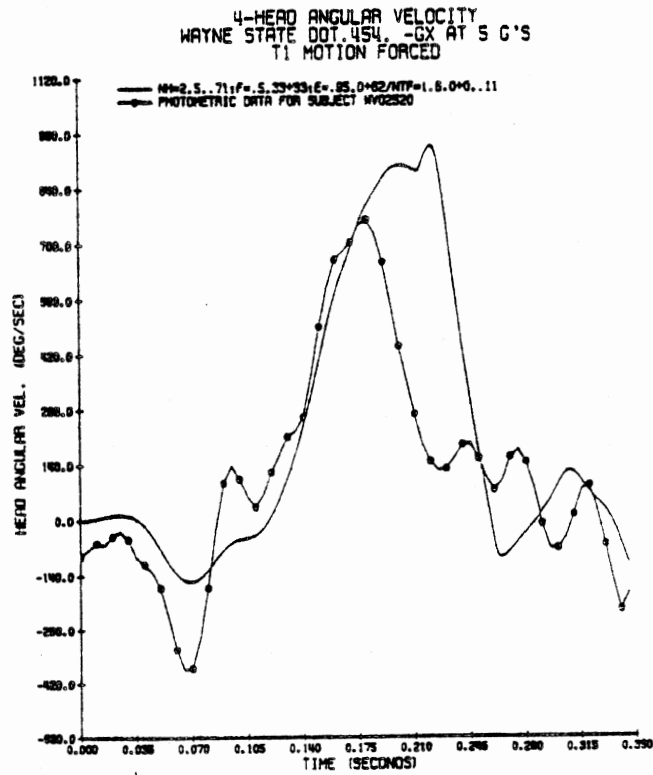


FIGURE 52. HEAD ANGULAR VELOCITY WITH INCREASED FLEXION STIFFNESS DOT454.

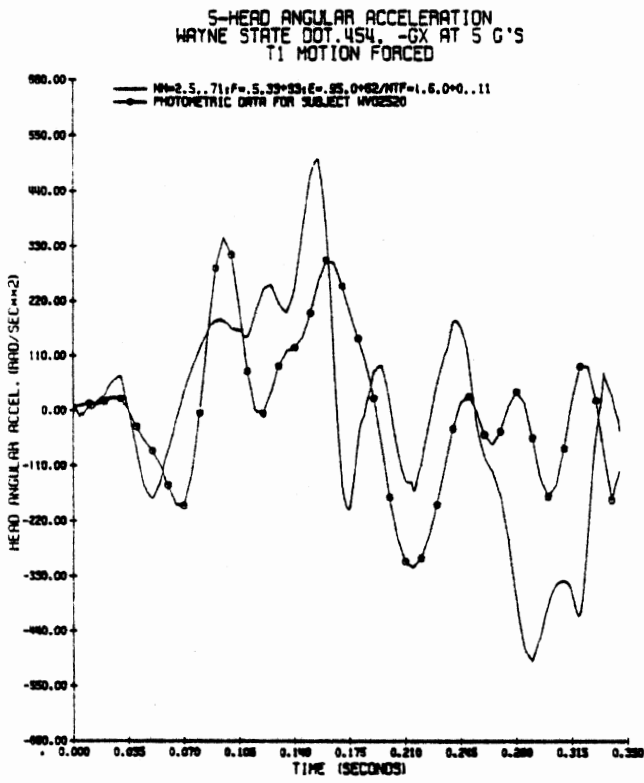


FIGURE 53. HEAD ANGULAR ACCELERATION FOR NBDL ADJUSTED FLEXION STIFFNESS DOT454.

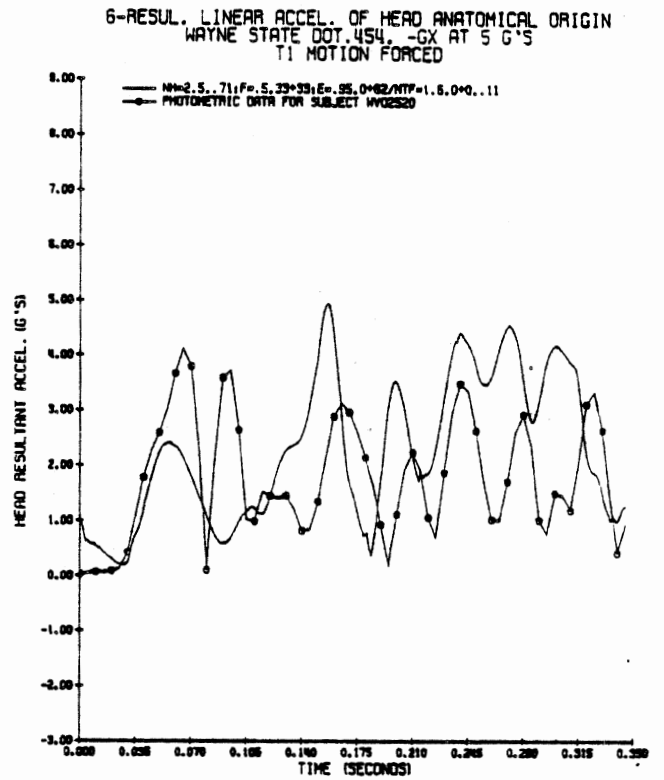


FIGURE 54. RESULTANT LINEAR HEAD ACCELERATION FOR NBDL ADJUSTED FLEXION STIFFNESS DOT454

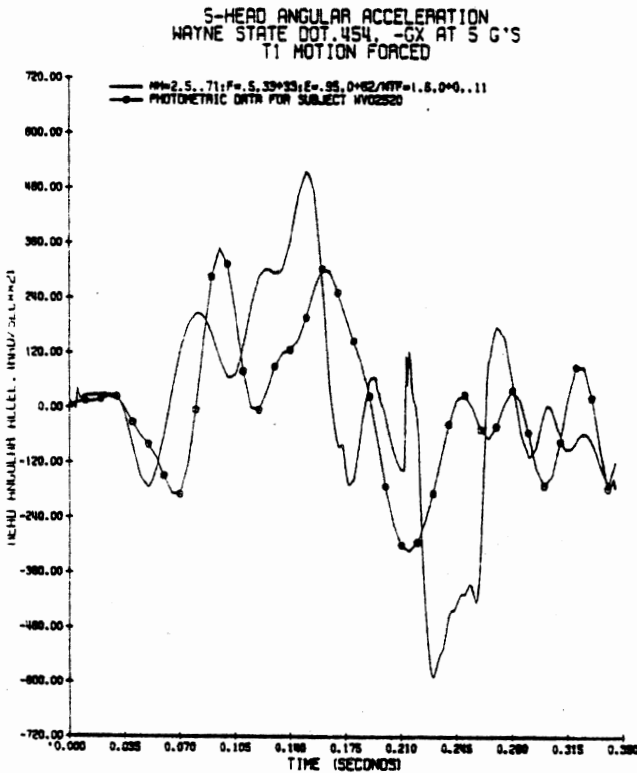


FIGURE 55. HEAD ANGULAR ACCELERATION FOR INCREASED FLEXION STIFFNESS DOT454.

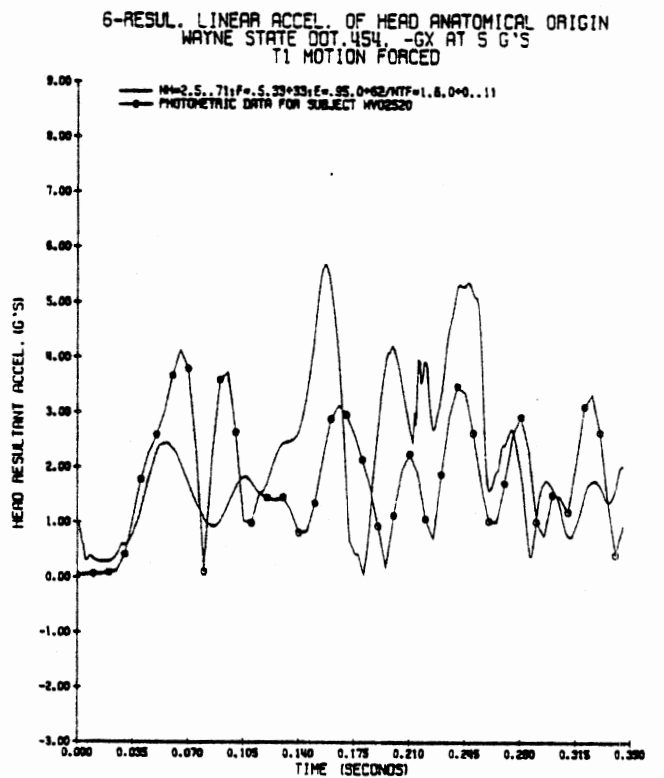


FIGURE 56. RESULTANT LINEAR HEAD ACCELERATION FOR INCREASED FLEXION STIFFNESS DOT454.

19-UPPER NECK MOMENT VS. ANGLE  
WAYNE STATE DOT.454, -GX AT 5 G'S  
T1 MOTION FORCED

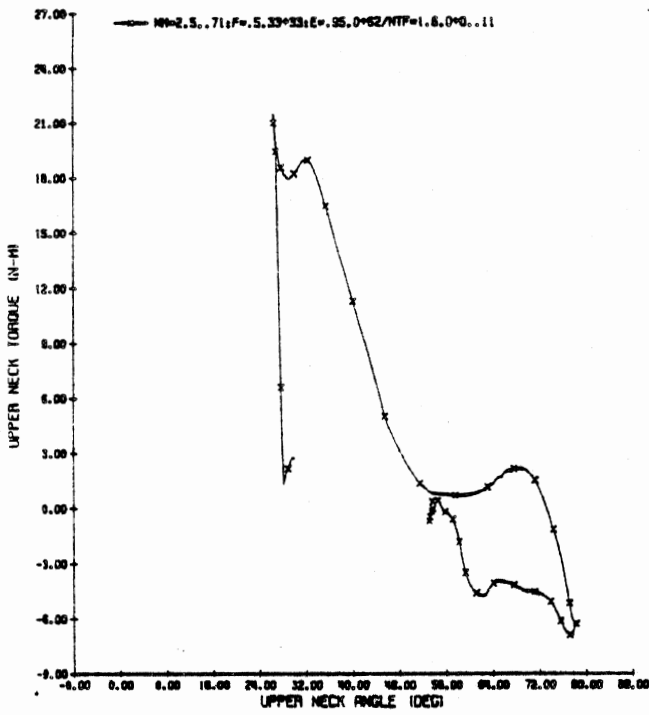


FIGURE 57. UPPER NECK MOMENT VS. NECK ANGLE FOR NBDL ADJUSTED FLEXION STIFFNESS DOT454.

20-LOWER NECK MOMENT VS. ANGLE  
WAYNE STATE DOT.454, -GX AT 5 G'S  
T1 MOTION FORCED

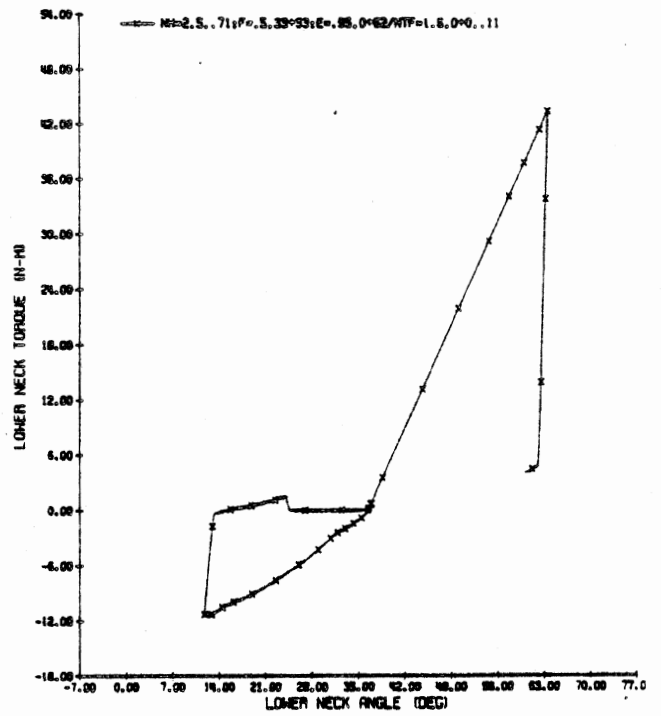


FIGURE 58. LOWER NECK MOMENT VS. NECK ANGLE FOR NBDL ADJUSTED FLEXION STIFFNESS DOT454.

19-UPPER NECK MOMENT VS. ANGLE  
WAYNE STATE DOT.454, -GX AT 5 G'S  
T1 MOTION FORCED

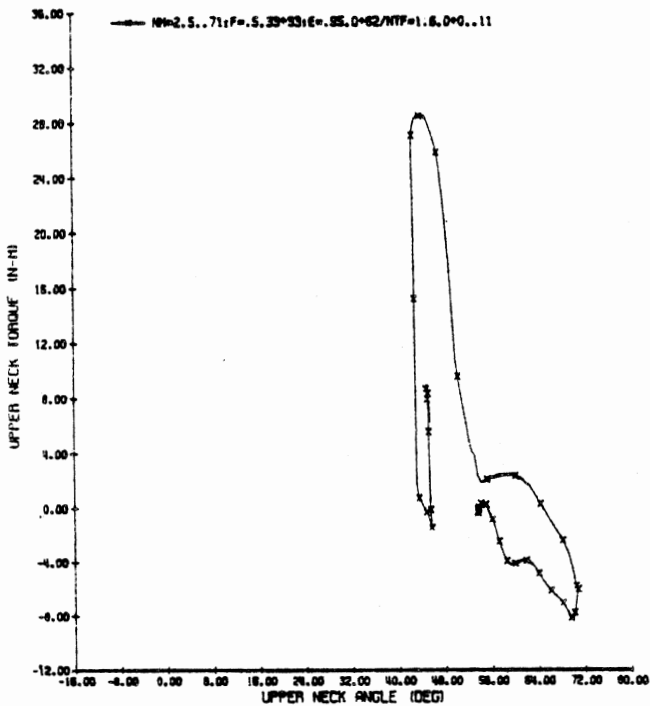


FIGURE 59. UPPER NECK MOMENT VS. NECK ANGLE FOR INCREASED FLEXION STIFFNESS DOT454.

20-LOWER NECK MOMENT VS. ANGLE  
WAYNE STATE DOT.454, -GX AT 5 G'S  
T1 MOTION FORCED

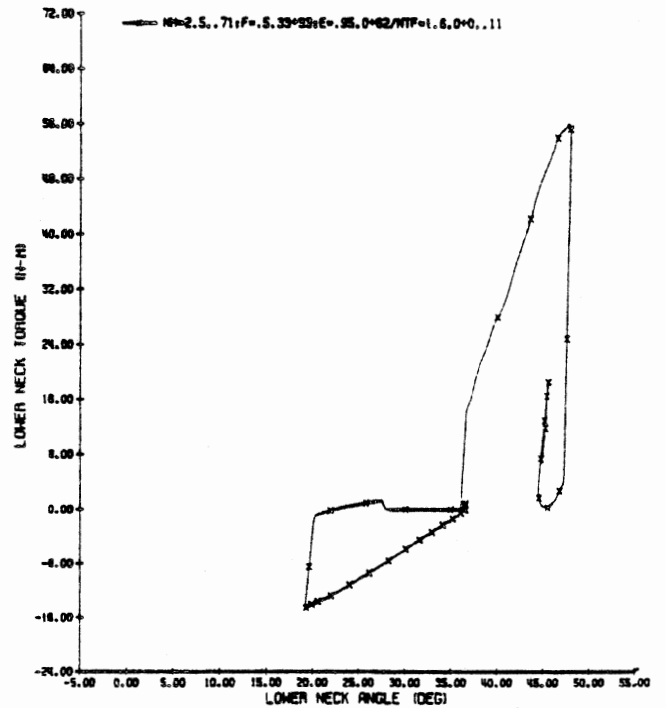


FIGURE 60. LOWER NECK MOMENT VS. NECK ANGLE FC INCREASED FLEXION STIFFNESS DOT454.

21-HEAD ANGLE VS. NECK ANGLE  
 MAYNE STATE DOT 345 -GX AT 5 G'S  
 T1 MOTION FORCED

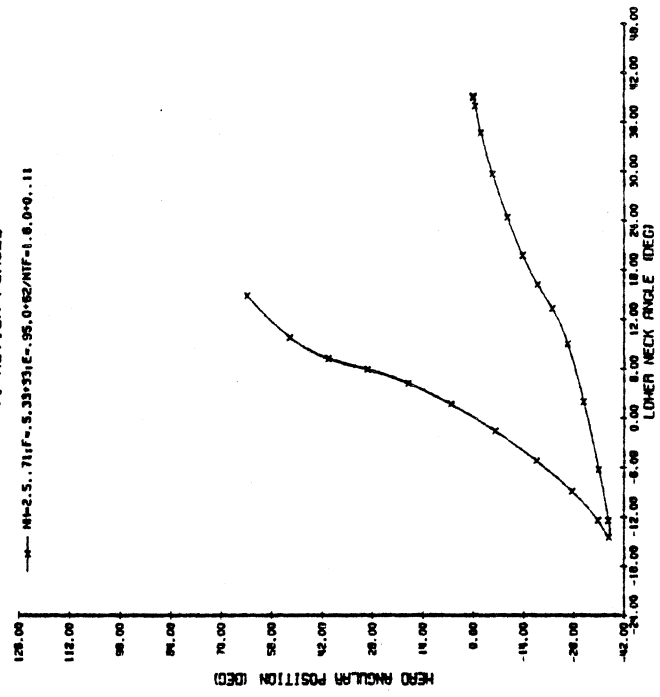


FIGURE 62. HEAD ANGLE VS. NECK ANGLE DOT345.

21-HEAD ANGLE VS. NECK ANGLE  
 MAYNE STATE DOT 331 -GX AT 20 G'S  
 T1 MOTION FORCED

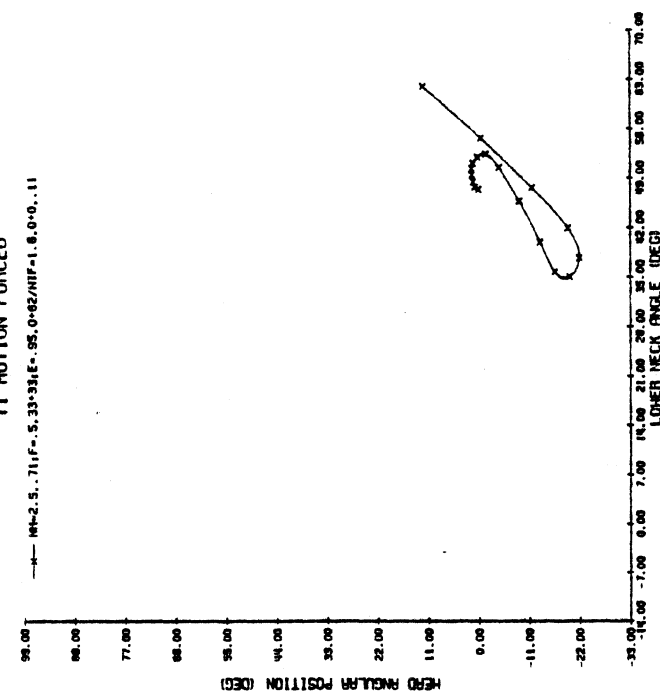


FIGURE 61. HEAD ANGLE VS. NECK ANGLE DOT331.

21-HEAD ANGLE VS. NECK ANGLE  
 WATNE STRIKE DOT. 308, -GX AT 5 G'S  
 TT MOTION FORCED

--- M=2.5, 711F=, 5.33\*331E-, 95, 0+62/MTF=1.0, 0+0, .11

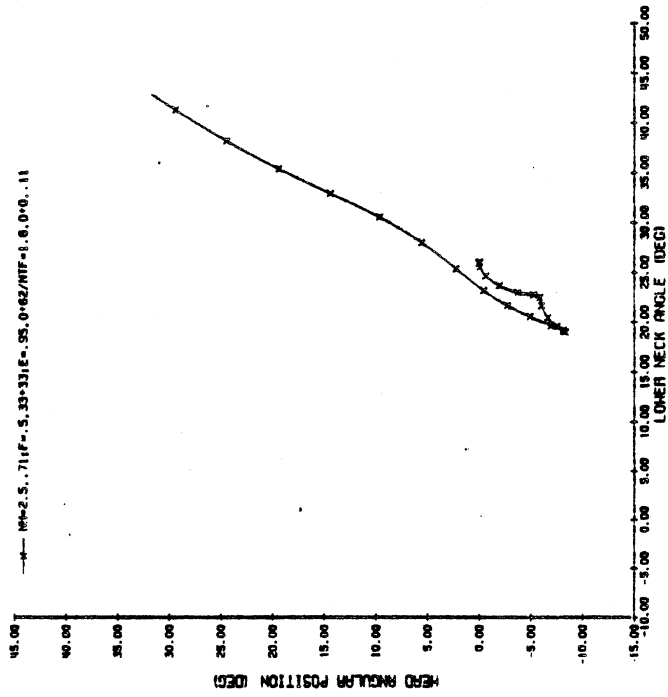


FIGURE 63. HEAD ANGLE VS. NECK ANGLE DOT308.

21-HEAD ANGLE VS. NECK ANGLE  
 WATNE STRIKE DOT. 453, -GX AT 5 G'S  
 TT MOTION FORCED

--- M=2.5, 711F=, 5.33\*331E-, 85, 0+62/MTF=1.0, 0+0, .11

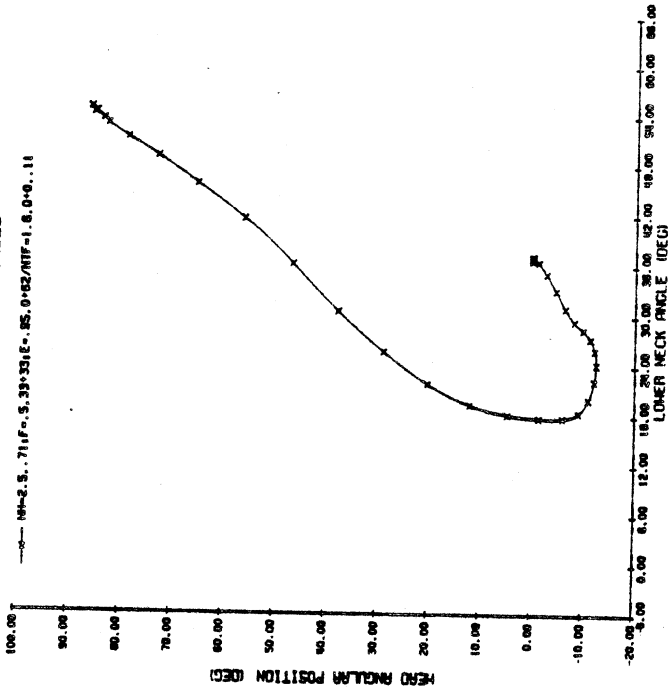


FIGURE 64. HEAD ANGLE VS. NECK ANGLE DOT453.

21-HEAD ANGLE VS. NECK ANGLE  
 WAYNE STATE DOT 454 - GX AT 5 G'S  
 Y1 MOTION FORCED

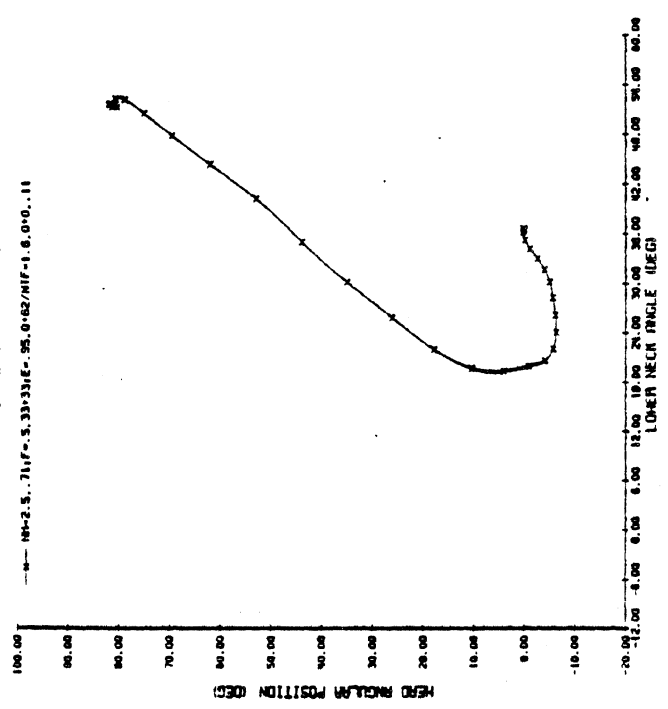


FIGURE 65. HEAD ANGLE VS. NECK ANGLE DOT454.

21-HEAD ANGLE VS. NECK ANGLE  
 WAYNE STATE DOT 455 - GX AT 5 G'S  
 Y1 MOTION FORCED

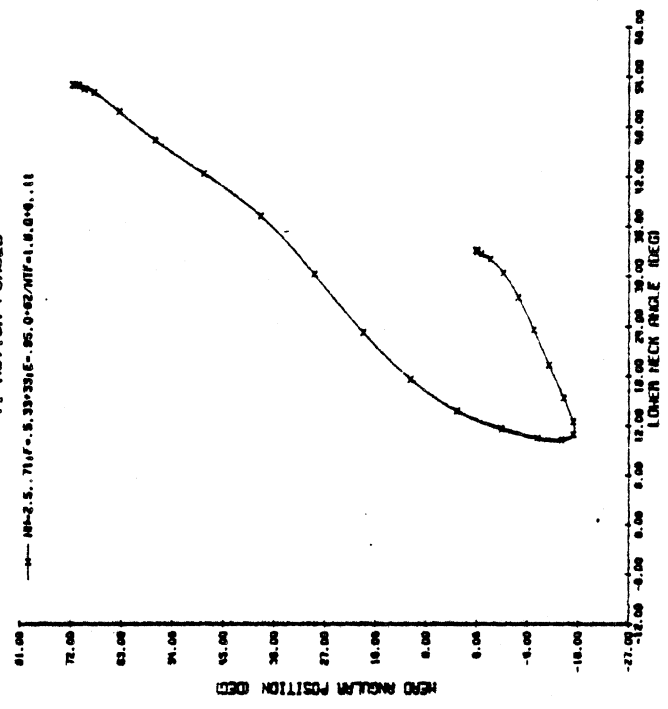


FIGURE 66. HEAD ANGLE VS. NECK ANGLE DOT455.

